Mutations in *Cog7* affect Golgi structure, meiotic cytokinesis and sperm development during *Drosophila* spermatogenesis

Giorgio Belloni[1,*], Stefano Sechi[1,*], Maria Giovanna Riparbelli[2], Margaret T. Fuller[3], Giuliano Callaini[2] and Maria Grazia Giansanti[1,‡]

[1]Istituto di Biologia e Patologia Molecolari del CNR, Dipartimento di Biologia e Biotecnologie Università di Roma Sapienza, P.le A Moro 5, 00185 Roma, Italy
[2]Dipartimento di Biologia Evolutiva, Università di Siena Via Aldo Moro 2, 53100 Siena, Italy
[3]Departments of Developmental Biology and Genetics, Stanford University School of Medicine, Stanford, CA 94305-5329, USA
*These authors contributed equally to this work
‡Author for correspondence (Mariagrazia.Giansanti@uniroma1.it)

Accepted 19 July 2012
Journal of Cell Science 125, 5441–5452

doi: 10.1242/jcs.108878

Summary

The conserved oligomeric Golgi (COG) complex plays essential roles in Golgi function, vesicle trafficking and glycosylation. Deletions in the human *COG7* gene are associated with a rare multisystemic congenital disorder of glycosylation that causes mortality within the first year of life. In this paper, we characterise the *Drosophila* orthologue of *COG7* (*Cog7*). Loss-of-function *Cog7* mutants are viable but male sterile. The Cog7 gene product is enriched in the Golgi stacks and in Golgi-derived structures throughout spermatogenesis. Mutations in the *Cog7* gene disrupt Golgi architecture and reduce the number of Golgi stacks in primary spermatocytes. During spermiogenesis, loss of the Cog7 protein impairs the assembly of the Golgi-derived acroblast in spermatids and affects axoneme architecture. Similar to the Cog5 homologue, four way stop (Fws), Cog7 enables furrow ingression during cytokinesis. We show that the recruitment of the small GTPase Rab11 and the phosphatidylinositol transfer protein Giotto (Gio) to the cleavage site requires a functioning wild-type *Cog7* gene. In addition, Gio coimmunoprecipitates with Cog7 and with Rab11 in the testes. Our results altogether implicate *Cog7* as an upstream component in a *gio-Rab11* pathway controlling membrane addition during cytokinesis.

Key words: *Drosophila*, Cog7, Cytokinesis, Golgi, Vesicle traffic

Introduction

The conserved oligomeric Golgi (COG) Complex is required for Golgi integrity, vesicle trafficking and glycosylation in yeast and mammalian cells (Smith and Lupashin, 2008; Ungar et al., 2006). Based on yeast genetics and electron microscopy, the COG complex was proposed to have a bi-lobed structure, with eight subunits (Cog1-8) arranged in two distinct subcomplexes: Lobe A (Cog1-4) and Lobe B (Cog5-8) (Loh and Hong, 2004; Ram et al., 2002; Ungar et al., 2002; Walter et al., 1998; Whyte and Munro, 2001). In yeast, subunits of Lobe A are essential components of the complex (VanRheenen et al., 1998; Whyte and Munro, 2001; Wuestehube et al., 1996), whereas Lobe B subunits are not substantially required for cell growth or internal membrane organisation (Ram et al., 2002; Whyte and Munro, 2001). Mutations in the genes encoding human *COG1*, *COG4-COG8* have been associated with congenital disorders of glycosylation (CDG) (Foulquier et al., 2006 Foulquier et al., 2007; Kranz et al., 2007; Lübbehusen et al., 2010; Ng et al., 2007; Paesold-Burda et al., 2009; Reynders et al., 2009; Spaapen et al., 2005; Steet and Kornfeld, 2006; Wu et al., 2004) indicating a role for COG in the transport and/or stability of Golgi glycosylation enzymes. Indeed studies in both yeast and mammalian cells have suggested that COG complex might function as a vesicle-tethering factor in intra-Golgi retrograde COPI transport (Ungar et al., 2002), thus regulating the distribution and the stability of Golgi resident proteins (Oka et al., 2004; Shestakova et al., 2006; Suvorova et al., 2001; Suvorova et al., 2002; Walter et al., 1998). A set of Golgi proteins called GEARs including giantin matrix proteins and glycosyltransferases/glycosidases were shown to mislocalize and to be abnormally degraded in Chinese hamster ovary (CHO) cells mutant for either Cog1 or Cog2 subunits (Oka et al., 2004). Depletion of Cog3 in HeLa cells resulted in the accumulation of COG complex-dependent (CCD) vesicles carrying Golgi v-SNARE proteins but no anterograde cargo molecules (Zolov and Lupashin, 2005). Consistent with a role in Golgi trafficking, COG subunits interact with intra-Golgi SNAREs, the COPI coat, small GTPases and other tethering proteins (Laufman et al., 2011; Sohda et al., 2007; Sohda et al., 2010; Suvorova et al., 2002).

Drosophila spermatogenesis provides a well suited model to study the requirement of Golgi trafficking *in vivo*, in a multicellular organism. Mutations in vesicle trafficking cause defects in various aspects of sperm development. For example, *Drosophila* spermatocytes are quite large cells (more than 20 μm in diameter), that complete two meiotic divisions in less than two hours (Fuller, 1993; Giansanti et al., 2012). Spermatocyte cytokinesis proved to be sensitive to mutations affecting vesicle traffic components (Brill et al., 2000; Farkas et al., 2003; Dyer

et al., 2007; Gatt and Glover, 2006; Giansanti et al., 2006; Giansanti et al., 2007; Polevoy et al., 2009; Robinett et al., 2009; Xu et al., 2002a; Zhou et al., 2011). During *Drosophila* spermiogenesis, round spermatids, ~12 μm in diameter, undergo drastic morphological changes in cell surface before reaching the impressive 1.8 mm in length of sperm tails (Fuller, 1993; Tates, 1971; Zhou et al., 2011). The 100-fold increase in cell length that characterises spermatid elongation is particularly dependent on membrane biosynthesis and membrane remodelling (Fabian et al., 2010; Farkas et al., 2003, Wei et al., 2008; Zhou et al., 2011). Among the COG subunits, the *Drosophila* Cog5 homologue Four way stop (Fws) has been implicated in both male meiotic cytokinesis and spermatid elongation (Farkas et al., 2003).

Here we have characterised the *Drosophila* orthologue of human Cog7. Loss of human COG7 is responsible for a rare, congenital disorder of glycosylation (CDG), namely CDG IIe (Morava et al., 2007; Ng et al., 2007; Wu et al., 2004). We show that mutants carrying null alleles of *Drosophila Cog7* are viable but male sterile. Cog7 function is essential to maintain Golgi structure and to regulate axoneme architecture during sperm development. Similar to Fws, Cog7 also controls furrow ingression during cytokinesis. Importantly, *Cog7* is required to localise the small GTPase Rab11 and the phosphatidylinositol transfer protein (PITP) Giotto (Gio) to the cleavage site of spermatocytes. In addition Gio coimmunoprecipitates with both Cog7 and Rab11 in *Drosophila* testes suggesting that these proteins may interact in male germ cells.

Results

Isolations of mutations in the *Drosophila Cog7* gene

Three mutant alleles of *Drosophila Cog7* were isolated by a cytological screen of the Zuker collection of male sterile lines (see Materials and Methods). Males homozygous for each allele and transheterozygotes carrying the allelic combinations $Cog7^{z\text{-}2805}$/$Cog7^{z\text{-}4495}$, $Cog7^{z\text{-}2805}$/$Cog7^{z\text{-}5797}$, $Cog7^{z\text{-}5797}$/$Cog7^{z\text{-}4495}$ are viable but male sterile. Mutant testes displayed frequent multinucleate spermatids suggesting failures in meiotic cytokinesis (Fig. 1A,B). Testes from *Cog7* males also exhibited a failure in spermatid elongation, a phenotypic trait previously observed in mutants in the *Drosophila* Cog5 homologue Fws (Fig. 1C) (Farkas et al., 2003).

All the mutations were uncovered by both *Df(3R)Exel6213* and *Df(3R)BSC861*. DNA sequencing revealed that each of the three mutant alleles carried nonsense mutations in the *CG31040* gene (Fig. 1D) encoding a 742 amino acid polypeptide that is homologous to human Cog7 (Ungar et al., 2002).

To determine the localisation of Cog7 in testes we generated transgenic flies expressing a GFP-Cog7 fusion protein. The *GFP-Cog7* transgene rescued both male sterility and the phenotypic defects associated with *Cog7* mutations indicating that the encoded protein is fully functional. In prophase I, GFP-Cog7 was enriched at multiple round structures that colocalized with the Golgi marker Lava Lamp (Lva, Sisson et al., 2000) indicating that Cog7 localises to the Golgi stacks (Fig. 2A). During metaphase and anaphase of meiosis I, GFP-Cog7 was associated with Golgi organelles in the polar regions of the cell (Fig. 2B,C). In telophase cells, Cog7 signals appeared excluded from the cell equator just like Lva-Golgi organelles (Fig. 2C,D; supplementary material Fig. S1). In onion-stage spermatids, Cog7 localised to Golgi derived acroblasts (Fig. 2E).

The subcellular localisation of Cog7 in spermatocytes is in accordance with the localisation of the Fws/Cog5 protein (Farkas et al., 2003) (Fig. 2F). To determine the functional dependence between Fws/Cog5 and Cog7, *Cog7* mutants expressing GFP-Fws

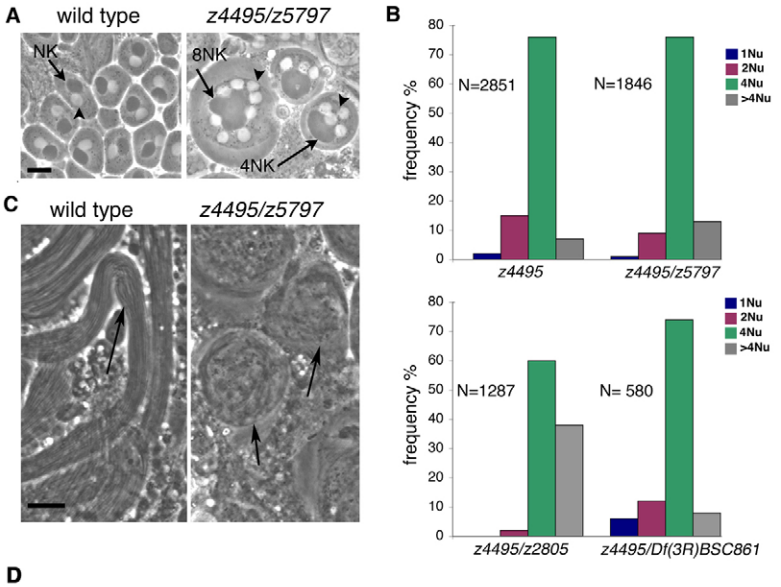

Fig. 1. Loss of *Cog7* disrupts spermatocyte cytokinesis and spermatid elongation. (**A**) Wild-type spermatids contain a single phase-light nucleus (arrowhead) and a phase-dark nebenkern (NK, arrow) of similar size. Most spermatids in *Cog7* display a large NK (4NK, arrow) and four normal-sized nuclei (arrowhead), indicating failure in cytokinesis during both meiotic divisions. Some *Cog7* spermatids contain a large nebenkern (8NK, arrow) and more than four nuclei (arrowhead), suggesting cytokinesis failure during both spermatogonial and spermatocyte divisions. Scale bar: 10 μm. (**B**) Frequencies of spermatids containing 1, 2, 4 or more than 4 nuclei per NK from *Cog7* mutant males. In the wild type, the frequency of multinucleate spermatids is virtually zero. (**C**) Cysts of elongated spermatids in wild-type (arrow) and ovoid cysts (arrows) of abnormally elongated spermatids in *Cog7*. Scale bar: 20 μm. (**D**) Amino acid sequence of *Drosophila* Cog7. Arrowheads indicate the positions of the stop codons in $Cog7^{z\text{-}4495}$ (red), $Cog7^{z\text{-}5797}$(blue) and $Cog7^{z\text{-}2805}$ (green).

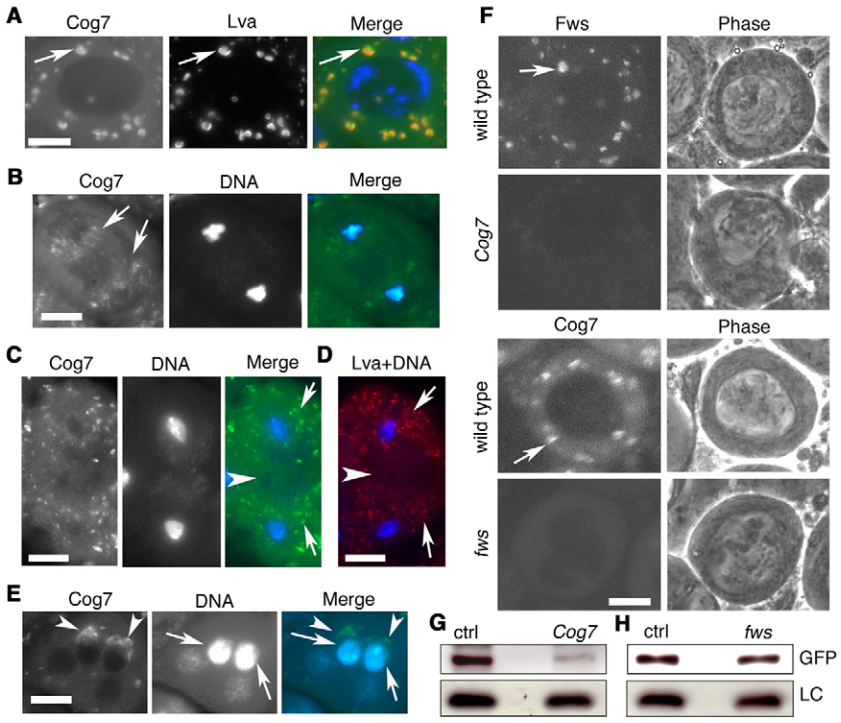

Fig. 2. Cog7 localises to Golgi in wild-type spermatocytes and spermatids. (**A**) Fixed prophase I spermatocyte expressing GFP-Cog7 (green) stained for Lva (red) and DNA (blue). Arrows point to Golgi stacks. (**B**) Fixed anaphase and (**C**) fixed telophase spermatocytes expressing GFP-Cog7 (green) stained for DNA (blue). Arrows point to Golgi membranes enriched in Cog7. (**D**) Fixed telophase spermatocytes stained for Lva (red) and DNA (blue). Arrows point to Golgi membranes enriched in Lva. Arrowheads in (C) and (D) indicate the cell midzones. (**E**) Spermatids expressing GFP-Cog7 (green) fixed and stained for DNA (blue). Arrows indicate nuclei, arrowheads indicate acroblasts. (**F**) Live wild-type and mutant spermatocytes expressing either GFP-Fws or GFP-Cog7 were imaged at the same exposure time. Arrows point to Golgi stacks. (**G**) Immunoblotting analysis of GFP-Fws in wild-type, GFP-Fws; $Cog7^{z3\text{-}4495}$/+(ctrl) and *Cog7* (GFP-Fws; $Cog7^{z\text{-}5797}/Cog7^{z\text{-}4495}$) mutant testes. Anti-Gio was the loading control (LC). (**H**) Immunoblotting analysis of GFP-Cog7 in wild-type, $fws^{z\text{-}0161}$/+; GFP-Cog7 (ctrl) and *fws* ($fws^{z\text{-}0161}/fws^{z\text{-}1201}$; GFP-Cog7) mutant testes. Anti-Gio was the loading control. Scale bars: 10 μm.

and *fws* mutants expressing GFP-Cog7 were examined. *Cog7* mutations completely abolished the localisation of Fws at the Golgi and Cog7 was diffuse in the cytoplasm in the absence of Fws (Fig. 2F).

Since Cog7 and Fws/Cog5 are believed to reside in the same COG subcomplex (Ungar et al., 2002), we assessed whether the stability of either protein was affected in the reciprocal mutant (Fig. 2G,H). Western blots showed that GFP-Cog5 protein was decreased by 56% in testes from *Cog7* mutants relative to wild type (Fig. 2G) and GFP-Cog7 protein was decreased by 20% in testes from *fws* mutants relative to wild type (Fig. 2H).

In order to verify whether other *Drosophila* putative COG proteins were also essential for male meiotic cytokinesis we used RNA interference (RNAi) induced by double stranded RNA (Dietzl et al., 2007). *Cog3* depletion resulted in frequent multinucleate spermatids suggesting that other COG components are required for spermatocyte cytokinesis (supplementary material Fig. S2).

Mutations in *Cog7* disrupt Golgi architecture and function in *Drosophila* spermatocytes

Because in mammalian cells, defects in COG subunits disturb Golgi architecture (Oka et al., 2005; Reynders et al., 2009; Ungar et al., 2002), we asked whether Cog7 is essential for maintaining Golgi integrity in *Drosophila* spermatocytes. Mature wild-type spermatocytes stained for Lva displayed multiple Golgi stacks of similar size (Fig. 3A,B). Conversely, in spermatocytes from *Cog7* males, most Lva signals appeared as small puncta (Fig. 3A) and the spherical structures were less numerous than in control cells (Fig. 3B). Similarly, in wild-type spermatocytes the Golgi Mannosidase II (GMII, Rabouille et al., 1999) concentrated in the Golgi stacks, whereas in *Cog7* the majority of this protein appeared associated with small puncta (Fig. 3C).

In wild-type mature spermatocytes analysed by transmission electron microscopy (TEM), the Golgi complex consisted of distinct clusters of membrane-bound compartments (Fig. 3D; n=42 cells analysed). Each Golgi stack was made of three to five flat disc-shaped cisternae, which were associated to abundant tubular-reticular networks and vesicles of various size. The edges of the disc-shaped cisternae bulged out in small vesicles and tubules. In *Cog7* spermatocytes the morphology of Golgi stacks was severely disrupted and Golgi consisted of clusters of irregularly sized and swollen cisternae (Fig. 3E,F; n=57 cells analysed).

Cog7 is required for contractile ring constriction during spermatocyte cytokinesis

Mutations in *fws* caused defects in F-actin ring constriction of telophase spermatocytes (Farkas et al., 2003). Staining of *Cog7* spermatocytes for tubulin and F-actin revealed a cytokinetic phenotype similar to *fws* (Fig. 4A). In 80% of mid-late telophases I from $Cog7^{z3\text{-}4495}$/*Df(3R)BSC861* (*Cog7*) mutants, the F-actin rings failed to constrict to completion and the central spindles appeared less dense than in wild type (n=25 for wild type; n=30 for *Cog7*; Fig. 4A). In order to further substantiate the phenotype of *Cog7*, we examined the localisation of Myosin II. Loss of function of Cog7 also resulted in failure to constrict the cortical ring of Myosin II complex proteins in telophase spermatocytes visualised by the *Drosophila* Myosin regulatory light chain Spaghetti Squash tagged with GFP (Sqh-GFP, Royou et al., 2002), or by anti Myosin II antibodies (Myo II, Royou et al., 2002). 74% of late telophases from *Cog7* males displayed defective Sqh-GFP rings (Fig. 4B; n=36 for wild type, n=34 for *Cog7*). Likewise, 79% of Myo II rings were large or broken during late telophase (Fig. 4C; n=60 for wild type, n=68 for *Cog7*).

Loss of Cog7 prevents the accumulation of G_{M1} to the cleavage site and affects the pattern of glycoconjugates at the cleavage equatorial membrane

COG subunit deficiencies are associated with defects in processing carbohydrate chains of both glycoproteins and glycolipids resulting in

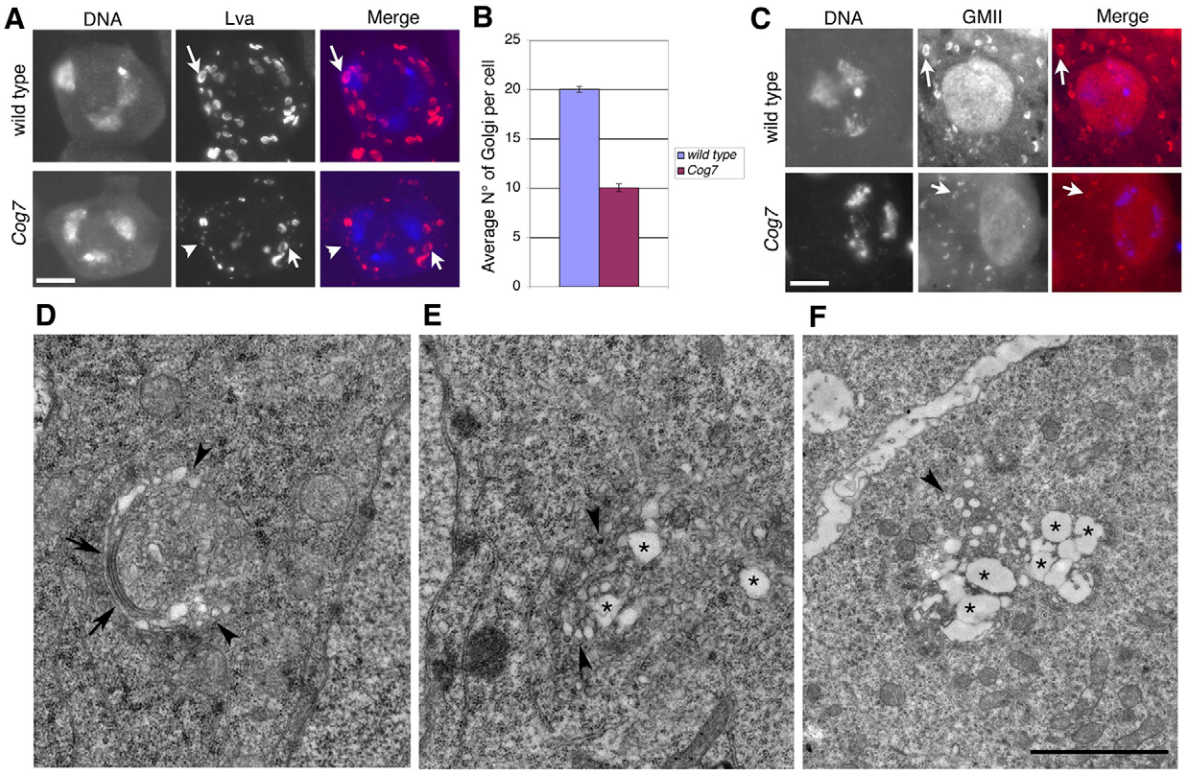

Fig. 3. Loss of Cog7 disrupts Golgi structure in primary spermatocytes. (**A**) Prophase primary spermatocytes were stained for Lva (red) and DNA (blue) Arrows point to Golgi stacks, arrowheads point to punctate signals. Scale bar: 10 µm. (**B**) The average number of Golgi stacks per cell (± SEM), visualised by Lva staining in prophase spermatocytes from wild type and Cog7 mutants. (**C**) Prophase primary spermatocytes were stained for GMII (red) and DNA (blue); Arrows point to Golgi stacks. (The bar represents 10 µm.) (**D–F**) Transmission electron microscopy (TEM) images show Golgi stacks (arrows) in nearly mature spermatocytes from (D) wild type and (E, F) *Cog7* mutants. Mutant Golgi display irregularly sized and swollen cisternae (asterisks) and a large number of vesicles (arrowheads in E and F). Scale bar: 2 µm.

altered cell surface glycoconjugates (Kingsley et al., 1986; Oka et al., 2005; Peanne et al., 2011; Reddy and Krieger, 1989; Ungar et al., 2006; Wu et al., 2004). We thus asked whether mutations in *Cog7* affected the pattern of glycoconjugates at the cleavage furrow.

Previous studies in sea urchin eggs revealed a unique equatorial membrane domain enriched in monosialotetrahexosylganglioside (G_{M1}), cholesterol and activated tyrosine kinases forms during late anaphase (Ng et al., 2005). By staining with fluorescent cholera

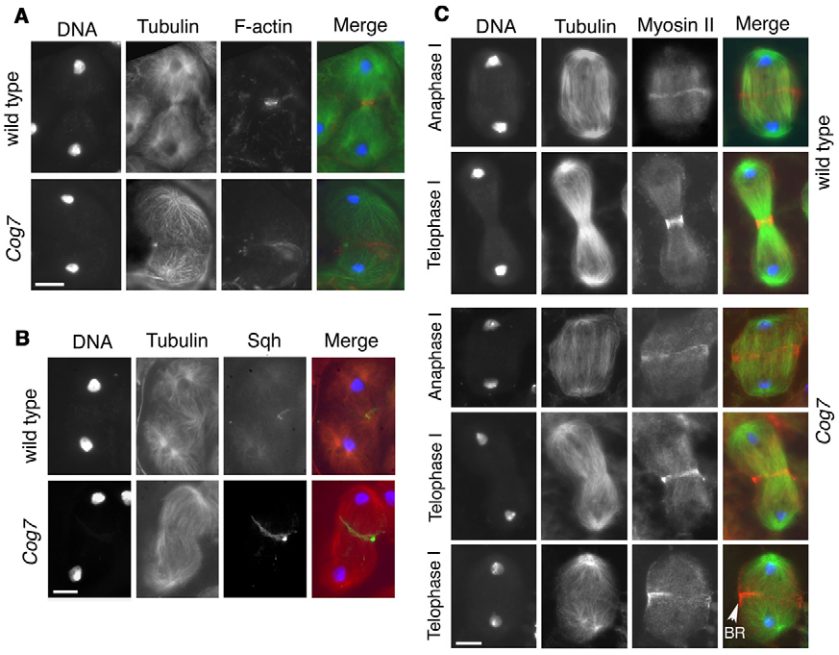

Fig. 4. Contractile ring constriction fails in *Cog7* spermatocytes. (**A**) Late telophase I stained for tubulin (green), F-actin (red) and DNA (blue). (**B**) Late telophase I expressing Sqh-GFP (green) and stained for tubulin (red) and DNA (blue). (**C**) Primary spermatocytes stained for myosin II (red), tubulin (green) and DNA (blue). Scale bars: 10 µm. BR, broken rings.

toxin subunit B (CTB), we found that G_{M1} accumulates in the furrow region of wild-type spermatocytes in late anaphase and telophase (Fig. 5A, $n=98$). Staining of *Cog7* spermatocytes failed to detect an accumulation of G_{M1} in 87% of late anaphase/telophase cells (Fig. 5A; $n=114$).

Glycoproteins with terminal sialic or N-acetylglucosamine residues concentrate in the cleavage furrow and can be visualised by staining with fluorescent wheat germ agglutinin (WGA) (Yoshigaki, 1997; Ng et al., 2005). Fluorescent WGA also stains the equatorial plasma membrane of *Drosophila* wild-type spermatocytes during late anaphase/telophase indicating an enrichment of sialic or N-acetylglucosamine glycoconjugates (Fig. 5B) (Giansanti et al., 2007) but failed to detect an accumulation of WGA receptors in all the *Cog7* cells examined (Fig. 5B, $n=80$ for wild type, $n=84$ for *Cog7*).

Wild-type function of Cog7 is required to recruit Giotto and Rab11 at the cleavage site

We examined whether loss of Cog7 affected the localisation of membrane traffic components involved in cytokinesis. Previous data showed that the phosphatidylinositol transfer protein (PITP) Giotto/Vib (Gio/Vib) and the small GTPase Rab11 accumulate at the cleavage site and are both required for spermatocyte cytokinesis (Gatt and Glover, 2006; Giansanti et al., 2006; Giansanti et al., 2007; Polevoy et al., 2009). It was suggested that Rab11, Gio and the Phosphatidylinositol 4-kinase β (PI4Kβ) Fwd function in the same pathway during cytokinesis, with Gio and Fwd acting upstream of Rab11 (Giansanti et al., 2007; Polevoy et al., 2009). Our immunofluorescence analysis revealed that loss of Cog7 impaired the recruitment of Gio at the cell equator in 89% of telophase spermatocytes (Fig. 6A; $n=32$ for wild type; $n=36$ for *Cog7*). *Cog7* mutations also disrupted the localisation of Rab11 in dividing spermatocytes. In both wild-type and *Cog7* prophase spermatocytes expressing Rab11-GFP, Rab11 was enriched at round structures corresponding to Lva-enriched Golgi stacks (supplementary material Fig. S3). Rab11-GFP colocalized with Lva in both wild-type and *Cog7* prophase cells. However, *Cog7* mutant spermatocytes displayed few Golgi organelles relative to wild-type control cells. In addition, Rab11 did not accumulate at the cell midzone in 90% of mutant telophases (Fig. 6B,C; $n=26$ for wild type; $n=30$ for *Cog7*). In contrast, the analysis of GFP-Cog7 distribution in *gio* and *Rab11* mutant spermatocytes revealed a normal localisation of this protein in both prophase and telophase (supplementary material Fig. S4). Since localisation of Rab11 to the cleavage site is dependent on both Gio (Giansanti et al., 2007) and Cog7 (this study) we performed Co-IP experiments using *Drosophila* testis protein extracts aimed at verifying interactions among these proteins. Protein extracts from testes expressing either GFP-Cog7 or Rab11-GFP were immunoprecipitated using the GFP-Trap (see Materials and Methods). We found that Gio coimmunoprecipitated with both Cog7 and Rab11 in *Drosophila* testes (Fig. 6D). Gio/Cog7 and Gio/Rab11 interactions were confirmed by a second experiment in which extracts from testes expressing Gio-RFP and either Rab11-GFP or GFP-Cog7 were immunoprecipitated using the RFP-Trap (Fig. 6E,F).

Because Gio coimmunoprecipitated with Cog7 in testis extracts, we asked whether the two proteins colocalized in dividing spermatocytes. To test this, we imaged spermatocytes expressing both GFP-Cog7 and Gio-RFP. Our analysis revealed that Gio partially colocalized with Cog7 at the Golgi membranes (Fig. 6G). Gio also localised to parafusorial and astral membranes where Cog7 was not detectable. In fixed dividing spermatocytes coexpressing Gio-RFP with Rab11-GFP, Gio colocalized with Rab11, consistent with previous results with anti-Gio and anti-Rab11 antibodies (supplementary material Fig. S5) (Giansanti et al., 2007). During telophase Gio and Rab11 concentrated at the cleavage furrow (Fig. 6A,B; supplementary material Fig. S5), while Cog7 was excluded from the cell equator (Fig. 2; supplementary material Fig. S1). In live preparations, Gio-RFP could be clearly detected on vesicles at the polar regions and in proximity of the cell equator (supplementary material Fig. S5).

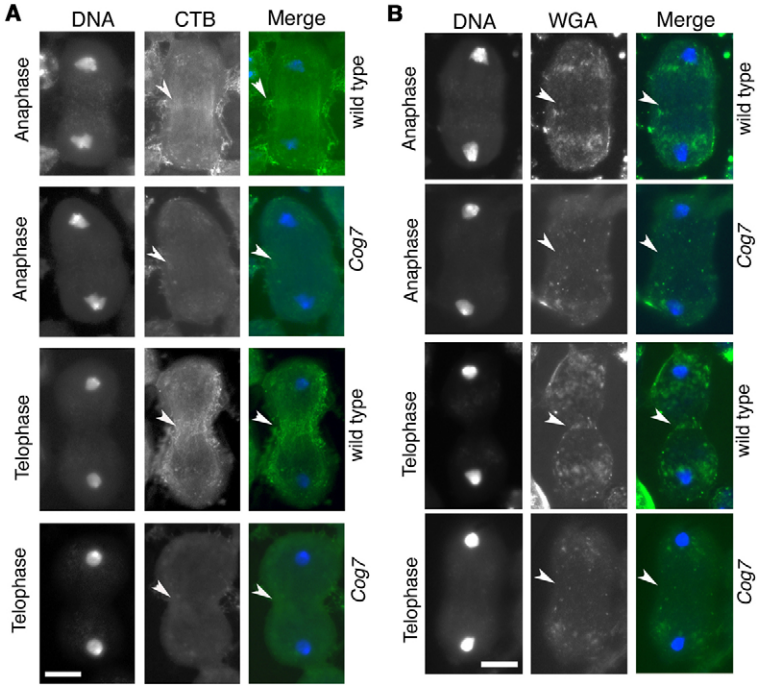

Fig. 5. Loss of Cog7 prevents the accumulation of G_{M1} to the cleavage site and affects the pattern of glycoconjugates at the cleavage equatorial membrane. (**A**) Late anaphase and telophase spermatocytes were fixed and stained with fluorescent cholera toxin subunit B (CTB) to detect G_{M1} (green) and with DAPI to detect DNA (blue). Arrowheads indicate the cell midzones. (**B**) Late anaphase and telophase spermatocytes were stained with fluorescent wheat germ agglutinin (WGA) (green) and with DAPI (blue). Arrowheads indicate the cell midzones. Scale bar: 10 µm.

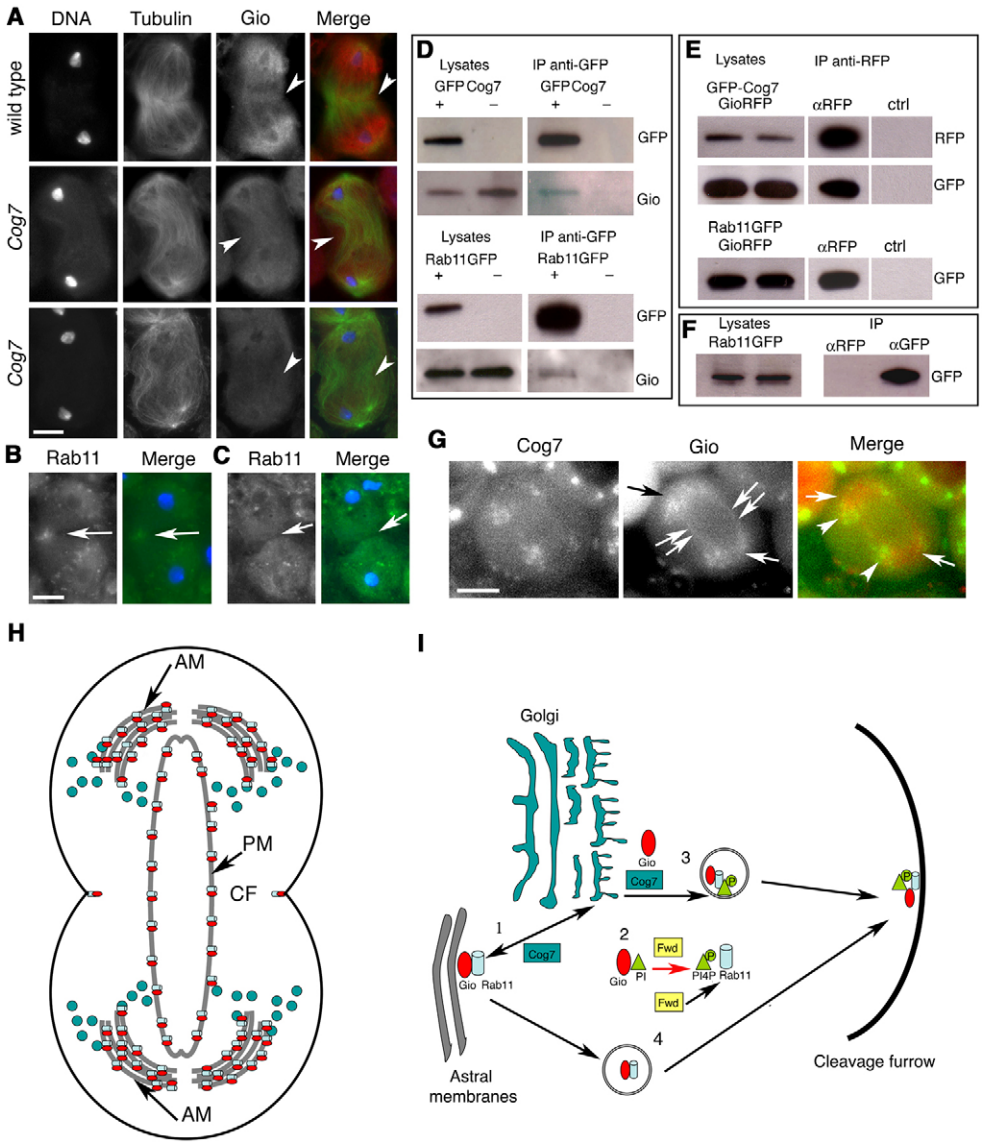

Fig. 6. Relationship between Cog7, Gio and Rab11 in dividing spermatocytes. (**A**) Gio fails to concentrate at the cell equator in *Cog7* telophase spermatocytes. Spermatocytes were stained with antitubulin (green), anti-Gio (red) and DAPI (blue). Arrows indicate the cell midzones. (**B**,**C**) Rab11 fails to localise at the cell midzone of *Cog7* telophase spermatocytes. Spermatocytes expressing Rab11-GFP (green) from (B) wild-type and (C) *Cog7* males were fixed and stained for DNA (blue). Arrowheads indicate the cell midzones. (**D**) Co-IP of Gio with Cog7 and Rab11. GFP-Cog7 and Rab11-GFP were immunoprecipitated from either GFP-Cog7 or Rab11-GFP transgenic testes with anti-GFP (i.e. GFP trap) and blotted with anti-Gio. The negative control was a wild-type no-transgenic stock. The left panels show the expression controls. (**E**) Gio-RFP was immunoprecipitated with anti-RFP (i.e. RFP trap) from transgenic testes expressing Gio-RFP and either GFP-Cog7 or Rab11-GFP. Equal fractions of testis extracts were incubated with RFP-trap beads (i.e. αRFP) or with control beads (ctrl). The left panels show the expression controls for the two fractions. (**F**) Equal fractions from Rab11-GFP testis extracts were used to test the specificity of the anti-RFP beads used in E. Rab11-GFP could be immunoprecipitated with anti-GFP beads (GFP trap, αGFP) but could not be immunoprecipitated with anti-RFP beads (RFP trap, αRFP). (**G**) Live dividing spermatocytes expressing GFP-Cog7 (green) and Gio-RFP (red) were imaged for GFP and RFP. In a fraction of the Golgi membranes, Gio partially colocalizes with Cog7 at the polar regions of dividing spermatocytes (arrowhead). Gio-RFP is also enriched at the astral membranes (arrows) and the parafusorial membranes (double arrows) that do not contain Cog7. (**H**) The diagram illustrates the localisation of Gio (red), Rab11 (light blue) and Cog7 (green) in telophase spermatocytes. (**I**) The diagram illustrates the possible functions of the Cog7-Rab11-Gio network during cytokinesis: (1) Cog7 might regulate retrograde/anterograde vesicle traffic between Golgi and ER astral/parafusorial membranes, thus contributing to target Gio and Rab11 to membrane compartments; (2) Gio provides the PI precursor for the synthesis of PI4P by Fwd on Golgi membranes; Fwd recruits Rab11 to the Golgi where it becomes associated with organelles containing PI4P; (3) Cog7 might also participate with Gio in the formation of secretory organelles that enrich the cleavage site; (4) Rab11 and Gio might also reach the cleavage site through vesicle traffic from the endoplasmic reticulum membranes to the CF. Scale bars: 10 μm. AM, astral membrane (in grey); CF, cleavage furrow; PM, parafusorial membrane (in grey).

Spermatids from *Cog7* males exhibit defects in acroblast assembly and in axoneme architecture

In wild-type onion-stage spermatids stained for Lva, the acroblast is a cone-shaped structure adjacent to the nucleus (Fig. 7A, $n=120$). In *Cog7* mutant spermatids, anti-Lva labelled numerous puncta but failed to detect a cone-shaped acroblast (Fig. 7A, $n=96$). Moreover immunostaining against the Golgi SNARE Syntaxin16 (Syx16, Xu et al., 2002b) revealed that this protein is

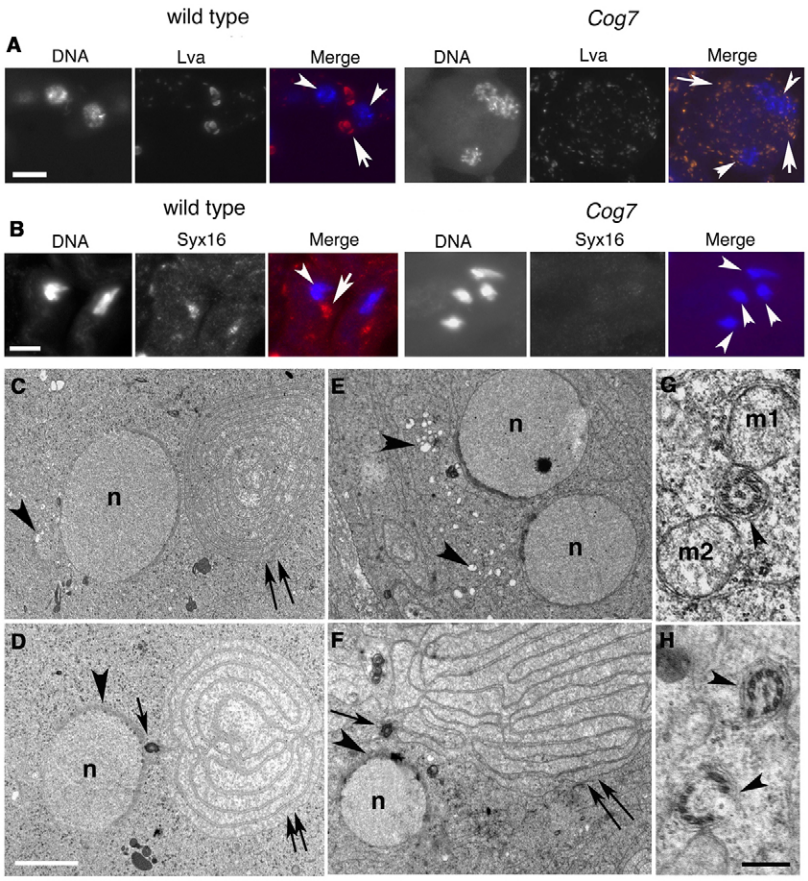

Fig. 7. Loss of Cog7 affects acroblast assembly in spermatids. (**A**) Onion-stage and (**B**) early elongating spermatids stained for DNA (blue) and either Lva (A, red) or Syntaxin 16 (B, red). Arrowheads point to nuclei and the arrows point to acroblasts in wild-type cells and point to Lva-enriched vesicles in *Cog7*. Scale bar; 10 μm. (**C–F**) Transmission electron microscopy (TEM) micrographs from (C,D) wild-type and (E,F) Cog7 onion-stage spermatids. Arrowhead in C indicates the wild-type acroblast in a juxtanuclear position; arrowheads in E indicate scattered vesicles that accumulate in mutant spermatids. The arrows in D and F point to basal bodies. The nuclei (n) and nuclear envelopes (arrowheads) are indicated. The basal body in the wild type is attached to the nuclear envelope. Double arrows indicate the nebenkern. Scale bar: 2 μm. (**G**,**H**) TEM micrographs show axonemes (arrowheads) in (G) wild-type and (H) mutant spermatids. m1 and m2 indicate mitochondrial derivatives. Scale bars: 200 nm.

enriched in wild-type acroblasts (n=60) but was entirely diffuse in mutant cells (Fig. 7B; n=54). TEM analysis confirmed failure to form acroblasts (Fig. 7C,E). In wild-type onion-stage spermatids, the acroblast was found in a juxtanuclear position (Fig. 7C; n=18 spermatids). *Cog7* mutant spermatids displayed numerous vesicles, scattered throughout the cytoplasm and lacked acroblasts (Fig. 7E; n=17 spermatids). TEM analysis revealed that loss of Cog7 also affects flagellar biogenesis. In wild-type onion-stage spermatids, the basal body was found attached to the surface of the nuclear envelope and an electron-dense adjunct formed a collar around this structure (Fig. 7D; n=37). In *Cog7* spermatids the structure of the basal body and the centriolar adjunct was not affected (Fig. 7F). However, 87% of basal bodies and centriolar adjuncts appeared displaced from the nuclear envelope, suggesting defects in basal body docking to the nuclear envelope (Fig. 7F; n=45). Cross sections of wild-type axonemes (Fig. 7G) revealed the typical organisation of axonemal microtubules into an arrangement composed of nine outer doublets and a central pair (9+2). Mutant spermatids were often defective in axoneme architecture. In our TEM studies, 25% of mutant axonemes appeared irregular in cross section and lacked peripheral doublets and/or central microtubules (Fig. 7H; n=97 mutant axonemes; n=131 control axonemes). These phenotypic defects were not specific for Cog7 mutants; similar, although less frequent aberrations were also observed in *gio* and *Rab11* mutant males (supplementary material Fig. S6). Axoneme architecture was disrupted in 18% of spermatids from *gio* males (n=273) and 15% of spermatids from *Rab11* males (n=213) (supplementary material Fig. S6).

Loss of Cog7 affects Golgi integrity in larval neuroblasts but has a weak effect on cytokinesis

Because *Cog7* null mutants are viable but male sterile we wondered whether Cog7 is required for Golgi integrity in cell types other than spermatocytes. In salivary glands and central nervous system (CNS) of larvae expressing GFP-Cog7, Cog7 localised on Golgi bodies (not shown). In wild-type interphase neuroblasts Lva concentrated in multiple Golgi bodies of similar size. In *Cog7* Lva-enriched structures were less numerous and appeared smaller than in wild type (Fig. 8). Golgi was also defective in mutant salivary gland cells (supplementary material Fig. S7). Given the defects in Golgi structure of *Cog7* mutants, we asked whether Cog7 protein is essential during mitotic divisions of larval neuroblasts. Analysis of larval brain squashes revealed a low frequency of tetraploidy: 3% of metaphases were tetraploid in *Cog7* (n=495 metaphases) versus 0% in wild type (n=510). Immunostaining of larval brains for Anillin also indicated mild defects during cytokinesis; 15% of mid-telophases from *Cog7* displayed poorly constricted or broken contractile rings (Fig. 8D–F). Loss of *Cog7* did not appear to affect other mitotic parameters; the mitotic index and the frequency of prometaphases/metaphases relative to all mitotic figures were not significantly increased in *Cog7* larval brain preparations (Fig. 8F).

Discussion

Wild-type function of the *Drosophila* homologue of Cog7, a subunit of the conserved octameric oligomeric complex (COG), involved in membrane trafficking and glycoconjugate synthesis

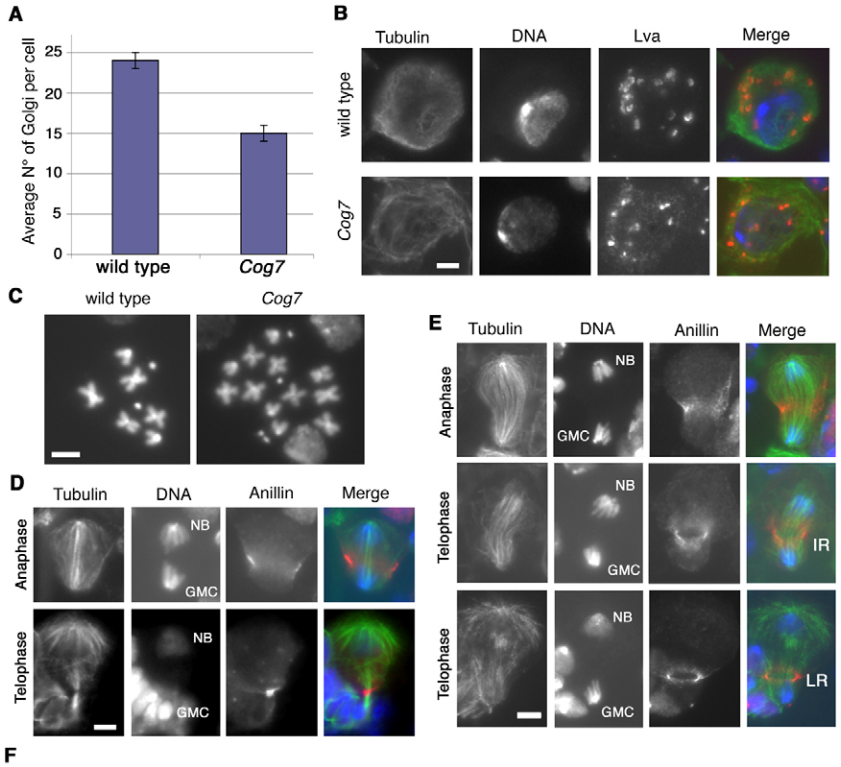

F

Genotype	Number of OF	Number of MF	% of Metaphases	MI	% of Irr.Telophases
Oregon-R	280	393	66	1.4	0*
Cog7	256	412	68	1.6	15§

Fig. 8. Loss of Cog7 affects Golgi structure but causes only mild defects in cytokinesis of larval neuroblasts. (**A**) Average number of Golgi per cell in interphase neuroblasts. (**B**) Neuroblasts during interphase stained for tubulin (green), Lva (red) and DNA (blue). (**C**) Normal female metaphase from wild-type and tetraploid female metaphase from *Cog7* in larval central nervous system (CNS). (**D**,**E**) Wild-type and *Cog7* mutant neuroblasts were stained for tubulin, anillin and DNA. (**F**) Mitotic parameters and percentage of irregular telophases (Irr. Telophases) in larval CNS from Oregon-R and *Cog7* mutants stained for tubulin, anillin and DNA. OF is the optic field, the circular area defined by a phase-contrast Neofluar 100× Zeiss objective, using 10× oculars and the Optovar set at 1.25; MF is the number of mitotic cells scored; MI is the mitotic index, the average number of mitotic figures per optic field. *n=75 scored; §n=93 scored. Scale bar: 5 μm. NB, neuroblast nucleus; GMC, ganglion mother cell nucleus. IR, irregular rings; LR, large rings that failed to constrict.

(Smith and Lupashin, 2008; Ungar et al., 2002; Ungar et al., 2006), is required for maintaining Golgi structure in both spermatocytes and spermatids. Studies in yeast and mammalian cells suggest a primary role for the COG complex in tethering retrograde vesicles that traffic within the Golgi (Bruinsma et al., 2004; Oka et al., 2004; Sohda et al., 2010; Suvorova et al., 2002; Zolov and Lupashin, 2005) and between endosomal compartments and the Golgi (Laufman et al., 2011; Smith et al., 2009; VanRheenen et al., 1999), thus contributing to the normal structure and function of the Golgi apparatus (Smith and Lupashin, 2008; Ungar et al., 2006). The dependence of other trafficking steps, such as endoplasmic reticulum (ER) export and ER-to-Golgi transport (VanRheenen et al., 1998; VanRheenen et al., 1999; Wu et al., 2004; Wuestehube et al., 1996) on Cog proteins may be secondary to a primary role in maintaining Golgi integrity and function.

Mutations in the genes encoding human *COG1*, *COG4-COG8* have been associated with congenital disorders of glycosylation (CDG) (Foulquier et al., 2006; Foulquier et al., 2007; Kranz et al., 2007; Lübbehusen et al., 2010; Ng et al., 2007; Paesold-Burda et al., 2009; Reynders et al., 2009; Spaapen et al., 2005; Steet and Kornfeld, 2006; Wu et al., 2004) suggesting a role for COG in the retention and/or retrieval of Golgi glycosylation enzymes. Indeed, loss of COG subunits impaired the localisation and the stability of Golgi resident proteins, which are known to recycle within the Golgi stacks (Oka et al., 2004; Zolov and Lupashin, 2005). In mammalian cells, deficiencies in COG subunits affect Golgi integrity causing several types of structural alterations. Depletion of Cog3 in HeLa cells caused fragmentation of the Golgi ribbon (Zolov and Lupashin, 2005), Cog1 and Cog2 CHO null mutants and Cog5-deficient HeLa cells displayed cisternal dilation (Oka et al., 2005; Ungar et al., 2002), fibroblasts from Cog7 and Cog8 patients exhibited fragmented and/or vesiculated stacks, undulated appearance of stacks and swollen cisternae (Reynders et al., 2009).

It was surprising that flies homozygous for null alleles of *Cog7* were viable, although males were sterile and displayed various defects during spermatogenesis, as mutations in the gene encoding human Cog7 are associated with a lethal congenital disorder of glycosylation (CDG), causing multisystemic deficiencies including neurological, metabolic and anatomical abnormalities (Morava et al., 2007; Ng et al., 2007; Wu et al., 2004).

Drosophila Cog7, along with the Cog5 homologue Fws, localised to Golgi throughout spermatogenesis. In addition Cog7 and Fws were interdependent for localisation to Golgi membranes. The organisation of Golgi into many stacks scattered throughout the cytoplasm in most *Drosophila* cells (Kondylis and Rabouille, 2009) allowed identification of subtle structural alterations in the *Cog* mutants that might have been missed in analysis of mutant mammalian cells, where Golgi stacks are interconnected into a pericentriolar ribbon. Loss of function of *Drosophila* Cog7 affected the integrity and the number of Golgi stacks in primary spermatocytes, as well as the structure of Golgi cisternae, consistent with previous EM studies in COG7 patient cells (Reynders et al., 2009) and in CHO cells carrying either Cog1 or Cog2 null mutations (Ungar et al., 2002; Vasile et al.,

2006). Loss of function of Cog7, like loss of function of *fws*, also disrupted assembly or stability of the Golgi-based acroblasts that form after meiosis II from Golgi-derived vesicles in onion-stage spermatids (Farkas et al., 2003; Giansanti et al., 2006; Giansanti et al., 2007).

Rather than fusing to form a compact juxtanuclear acroblast, Cog7 mutant Lva-containing vesicles were scattered and the Golgi SNARE Syntaxin16 (Syx16, Xu et al., 2002b) was entirely diffuse in mutant cells. Based on these data, the defects in acroblast formation might be a consequence of a failure to recruit Syntaxin proteins to Golgi organelles at the end of meiosis, thus impairing Golgi membrane fusion. Consistent with a role for the Cog proteins in recruiting Syntaxin proteins, it has been recently demonstrated that loss of function of Cog6 in HeLA cells abrogated the steady state level of Syntaxin 6, markedly reduced localisation of Syntaxin 16 to Golgi membranes and impaired the assembly of the Syntaxin 6-Syntaxin 16-Vti1a-VAMP4 SNARE complex (Laufman et al., 2011).

Cog7 mutant males displayed defects in cell elongation in differentiating spermatids, similar to *fws* and *syntaxin 5* mutants. Spermatid elongation, which involves a 100-fold increase in cell surface area, may necessitate the addition of new membrane derived from Golgi vesicles and so may be especially sensitive to defects in Golgi structure and/or function (Fabian et al., 2010; Farkas et al., 2003; Fuller, 1993; Tates, 1971; Wei et al., 2008; Zhou et al., 2011). In addition, loss of Cog7 affected architecture of the developing flagellar axonemes and resulted in dissociation of the basal body from the nuclear envelope, suggesting defects in the docking to the nuclear envelope. These defects were not specific for *Cog7*; similar although less frequent alterations were also observed in *gio* and *Rab11* males.

Recent studies demonstrated that depletion of the phosphoinositide phosphatidylinositol 4,5 biphosphate (PIP2) results in defects in both axoneme architecture and in basal docking to the nuclear envelope (Wei et al., 2008). However, axonemal of PIP2-depleted flies also exhibited alterations not observed in *Cog7* flies, such as triplets as well as doublets among outer microtubules, suggesting a role for PIP2 or a downstream second messenger in controlling the transition from basal body to axonemal microtubule arrays (Wei et al., 2008). The defects in axoneme architecture are not merely the consequence of cytokinesis failure, as other mutants defective in cytokinesis form regular axonemes (Wei et al., 2008). Further investigations will be necessary to clarify whether *Cog7* defects in flagellar biogenesis are the consequence of Golgi malfunction.

Function of Cog7, like the Cog5 homologue Fws (Farkas et al., 2003), is essential for successful cytokinesis in *Drosophila* spermatocytes. Cytokinesis involves a rapid and massive expansion in plasma membrane surface area that strongly depends on endocytic and/or secretory membrane trafficking pathways in several cell systems (Albertson et al., 2005; Boucrot and Kirchhausen, 2007; McKay and Burgess, 2011; Neto et al., 2011; Prekeris and Gould, 2008). Previous studies have demonstrated that spermatocyte cytokinesis is sensitive to Brefeldin A (Robinett et al., 2009) and requires the wild-type function of the Golgi proteins Syntaxin 5 (Xu et al., 2002a), Fws (Farkas et al., 2003), Fwd (Polevoy et al., 2009) and Brunelleschi (Robinett et al., 2009), indicating a requirement for effective Golgi trafficking. The defective morphology of Golgi stacks in mutant spermatocytes strongly suggests that the failure of cytokinesis in *Cog7* mutant spermatocytes might be a consequence of defects in Golgi trafficking and/or function.

Previous studies showed that the phosphatidylinositol transfer protein (PITP) Giotto/Vib (Gio/Vib) and the small GTPase Rab11 concentrate to the cleavage furrow and are both required for spermatocyte cytokinesis (Gatt and Glover, 2006; Giansanti et al., 2006; Giansanti et al., 2007; Polevoy et al., 2009). Rab11, Gio and the Phosphatidylinositol 4-kinase β (PI4Kβ) Fwd might function in the same pathway controlling membrane addition to the spermatocyte cleavage site, with Gio and Fwd acting upstream of Rab11 (Giansanti et al., 2007). Fwd is required for the synthesis of PI4P on Golgi membranes and for the formation of Rab11-and PI4P containing organelles at the cell equator (Polevoy et al., 2009). Because PITPs can stimulate vesicle budding from the trans-Golgi network and also provide vesiculating activity for scission of coatomer-coated vesicles *in vitro* (Jones et al., 1998; Ohashi et al., 1995; Simon et al., 1998) Gio might be involved in vesicle formation. We found that localisation of Gio and Rab11 to the cleavage furrow in dividing spermatocytes requires the wild-type function of Cog7, indicating that Cog7 might be an upstream component in a *gio-Rab11* pathway during cytokinesis (Fig. 6I). Gio coimmunoprecipitates with both Rab11 and Cog7 in testes, suggesting that these proteins may form a complex in male germ cells. Based on our results, Cog7 might be implicated in the Gio-mediated formation of Rab11 associated secretory organelles which become enriched in the cleavage site during spermatocytes (Fig. 6H,I). However, we cannot exclude a role for Cog7 and the Cog complex in the regulation of a retrograde/anterograde traffic between Golgi membranes and ER during cytokinesis (Fig. 6I).

In addition to defects in recruitment of membrane trafficking proteins, *Cog7* mutant spermatocytes also exhibited incomplete actomyosin ring constriction, as also observed in *fws* (Farkas et al., 2003), *gio* (Giansanti et al., 2004; Giansanti et al., 2006), *fwd* (Giansanti et al., 2004) and *Rab11* (Giansanti et al., 2007) mutant spermatocytes. Although regular actomyosin rings formed during early telophase, they failed to contract during cytokinesis. Several studies have indicated that actomyosin ring assembly and remodelling during cytokinesis is strictly dependent on membrane trafficking during furrowing. For example in *Dictyostelium*, clathrin-minus cells fail to assemble myosin II into a functional contractile ring and mutations in *syntaxin1* disrupt actin organisation during furrow formation of *Drosophila* embryos (Niswonger and O'Halloran, 1997; Burgess et al., 1997). Interestingly, live analysis of fluorescent tagged vesicles and F-actin movement during cytokinesis of postcellurized *Drosophila* embryos has suggested a model in which actin and membrane are delivered as a unit to the invaginating furrows (Albertson et al., 2008).

A possible explanation for how loss of Cog7 could affect contractile ring constriction is suggested by result that fluorescent WGA receptors concentrate at the equatorial site of telophase cells in wild type but not in *Cog7* mutants, indicating a defect in the accumulation of glycoproteins with terminal sialic or N-acetylglucosamine residues. We speculate that particular glycoproteins must be enriched at the equatorial site to control the contraction of the actomyosin ring during cytokinesis. Mutations in *Cog7* might affect glycosylation in the Golgi and so impair localisation of these glycoproteins at the cell surface, resulting in failure of ring constriction. CHO cells deficient for either Cog1 or Cog2 exhibit defects in Golgi-associated processing reactions for the synthesis of N-linked, O-linked

carbohydrate chains of glycoproteins and also glycolipids (Kingsley et al., 1986). Consistent with a requirement for the COG complex in processing lipid-linked carbohydrate chains, an enrichment of the ganglioside G_{M1} could be visualised in telophase spermatocytes stained with fluorescent CTB in wild type but not in *Cog7* mutants.

Previous work in sea urchin showed that a membrane equatorial domain, enriched in G_{M1} cholesterol and signalling molecules, forms during late anaphase with the contractile ring and suggested the existence of signalling platforms that control cytokinesis (Ng et al., 2005). Thus, failure to localise G_{M1} might disrupt the structure of a special lipid raft domain in dividing spermatocytes and affect several aspects of cytokinesis such as the activation of signalling pathways that regulate furrowing, actin remodelling and membrane traffic.

Despite its fundamental role in spermatogenesis and spermatocyte cytokinesis, Cog7 was not essential for normal development in *Drosophila*. Karyotyping of mitotic chromosomes in larval brain cells from *Cog7* revealed a low frequency of tetraploidy and immunostaining indicated regular furrow ingression in 85% of telophases. Analysis of Golgi in mutant neuroblasts indicated a requirement for Cog7 in Golgi integrity also in these cells. However, loss of Cog7 and the consequent Golgi defects did not substantially affect cytokinesis of neuroblasts. Other mutations in membrane traffic components such as *fwd*, *fws*, *bru*, *gio* and *Arf6* disrupt spermatocyte cytokinesis causing little or no effects on cytokinesis of larval neuroblasts or S2 cells (Brill et al., 2000; Eggert et al., 2004; Farkas et al., 2003; Giansanti et al., 2004; Giansanti et al., 2006; Dyer et al., 2007; Robinett et al., 2009). The large size of spermatocytes and the rapid succession of two meiotic divisions might explain the particular requirement of male meiotic cytokinesis for vesicle trafficking pathways.

Materials and Methods

Fly strains and transgenes

$Cog^{z\text{-}4495}$, $Cog^{z\text{-}5797}$ and $Cog^{z\text{-}2805}$ alleles of *Drosophila Cog7* were obtained by screening the C. Zuker collection of male sterile lines (Wakimoto et al., 2004; Giansanti et al., 2004). Chromosomal deficiencies *Df(3R)BSC861* and *Df(3R)D1-BX12* were obtained from the Bloomington *Drosophila* Stock Center at Indiana University. Flies carrying the *four way stops* (*fws*), *giotto* (*gio*) and *Rab11* mutations fws^{Z0161}, fws^{Z1201}, $gio^{RM1\text{-}r7}$, $gio^{z3\text{-}3934}$, gio^{EP513}, $Rab11^{e(To)3}$ and $Rab11^{93Bi}$ and flies expressing GFP-Fws have been described previously (Farkas et al., 2003; Giansanti et al., 2006). *UAS::DCog3-RNAi* flies were from the Vienna Drosophila RNAi Collection (VDRC). Flies expressing GAL4 (used to inactivate *Cog3* or to drive the expression of Gio-RFP from the *UAS-gio-RFP* transgene) were as follows: Bam-GAL4 (Chen and McKearin, 2003), gift of J. Wakefield (University of Exeter, UK); P{tubP-GAL4}LL7 (tub-GAL4) obtained from the Bloomington Stock Center, P{tubP-GAL4}LL7 $gio^{RM1\text{-}r7}$ (described in Giansanti et al., 2006). Flies expressing Rab11-GFP (Dollar et al., 2002) were a gift from R. S. Cohen (University of Kansas); flies expressing Sqh-GFP (Royou et al., 2002) were a gift from R. E. Karess (CNRS, University of Paris Diderot). To construct GFP-Cog7; gio^{z3934}/*Df(3R)D1-BX12* and GFP-Cog7; $Rab11^{e(To)11}$/$Rab11^{93Bi}$ mutant strains, *GFP-Cog7* (see below) was crossed into the *gio* and *Rab11* mutant background.

Molecular biology and rescue experiments

To generate the *GFP-Cog7* construct, the *EGFP* CDS was fused in frame to the N-terminus of the full length *CG31040* cDNA and cloned into the transformation vector pJZ4 (provided by G. D. Raffa; Raffa et al., 2010) under the control of a tubulin promoter. The Gateway strategy (Invitrogen) was used to generate the *UAS-gio-RFP* construct; full length *gio* cDNA (Giansanti et al., 2006) was cloned into the transformation vector pPWR (DGRC, Indiana University) that contains the Gateway cassette, the UASp promoter and the C-terminal monomeric red fluorescent protein (mRFP) sequence. Germline transformation was performed by Bestgene, Inc. (Chino Hills, CA). *GFP-Cog7* was crossed into the *Cog7* mutant background to test for phenotypic rescue of male sterility and meiotic cytokinesis failures. To verify whether the *UAS-gio-RFP* transgene could rescue *gio* mutations, females of genotype *w; UAS-gio-RFP; P{tubP- GAL4}LL7* $gio^{RM1\text{-}r7}$/*Tm6B* were crossed to *w/Y; Df(3R)D1-BX12/Tm6B* males and the progeny was scored for viability and fertility.

Microscopy and immunofluorescence

Cytological preparations were made with testes, brains or salivary glands from third instar larvae. $Cog7^{z\text{-}4495}$/*Df(3R)BSC861* mutants were used in all the experiments involving *Cog7* mutations except the ones described in Fig. 1. To visualise α tubulin with either Rab11-GFP or Sqh-GFP or to stain F-actin with Rhodamine-phalloidin (Molecular Probes) larval testes were fixed in 4% formaldehyde as described in Giansanti et al. (Giansanti et al., 2006). For other immunostaining with testes or larval brains, preparations were fixed using 3.7% formaldehyde in PBS and then squashed in 60% acetic acid according to Giansanti et al. (Giansanti et al., 1999). To visualise mitotic chromosomes, larval brains were dissected in NaCl 0.7%, treated with hypotonic solution for 7′, fixed in 45% acetic acid, processed as per Giansanti et al. (Giansanti et. al., 1999) and mounted in Vectashield medium with DAPI (Vector Laboratories, Burlingame, CA). Salivary glands from third-instar larvae were dissected in PBS and fixed in 4% formaldehyde for 10′. Monoclonal antibodies were used to stain α tubulin (T6199, Sigma-Aldrich, diluted 1:200). Polyclonal antibodies were as follows: anti-Myosin II (Royou et al., 2002), gift from R. E. Karess, diluted 1:400; rabbit anti Anillin (Field and Alberts; 1995), gift from C. Field (Harvard Medical School), diluted 1:300; rabbit anti-Lava Lamp (anti-Lva, Sisson et al., 2000), gift from O. Papoulas (University of Texas), diluted 1:500; rabbit anti Mannosidase II (anti-dGMII, Rabouille et al., 1999), gift from D. B. Roberts, diluted 1:200; rabbit anti-Gio (Giansanti et al., 2006) diluted 1:3000; rabbit anti-dSyntaxin16 (antidSyx16, Xu et al., 2002b), gift from W. Trimble (University of Toronto), diluted 1:20. For staining with fluorescein-labelled cholera toxin B subunit (Sigma-Aldrich, C1655, diluted 1:200) or with FITC-conjugated wheat germ agglutinin (WGA, Molecular Probes) testes preparations were fixed according to Giansanti et al. (Giansanti et. al., 1999). Secondary antibodies Alexa 555-conjugated anti rabbit IgG (Molecular Probes) and rhodamine/FITC-conjugated anti-mouse IgG (Jackson Immunoresearch, West Grove, PA), were used at 1:250 and 1:20 respectively. In all cases slides were mounted in Vectashield medium with DAPI. Images were captured with a charged-coupled device (CCD camera, Photometrics Coolsnap HQ), connected to a Zeiss Axioplan, epifluorescence microscope, equipped with an HBO 100-W mercury lamp, and 40× or 100× objectives as described in Giansanti et al. (Giansanti et al., 2006).

Areas of Golgi bodies were measured using image J (NIH; http://rsbweb.nih.gov/ij/).

Transmission electron microscopy

Testes from both mutant and control larvae or pupae were dissected in PBS and fixed overnight at 4℃ in 2.5% glutaraldehyde in PBS. After two rinses (2×20 minutes) in PBS, specimens were post-fixed in 1% osmium tetroxide in PBS for 2 hours. Preparations were then washed for 30 minutes in PBS and for 30 minutes in distilled water, dehydrated through a series of graded ethyl alcohols and then embedded in an Epon-Araldite mixture and polymerized at 60℃ for 48 hours. Ultrathin sections, obtained with a LKB ultratome Nova, were collected on Formvar copper coated grids and stained with uranyl acetate and lead citrate. Samples were then observed with a Philips CM 10 operating at 80 kV. Full serial 400 nm sections through the nuclear region were collected on copper Gilder slot grids, 2×1 mm, coated with Formar. Only selected sections were shown in the figures.

Live imaging

Larval testes were prepared for time lapse as per Inoue et al. (Inoue et al., 2004) and imaged as described in Giansanti et al. (Giansanti et al., 2006). Spermatocytes were examined with a Zeiss Axiovert 20 microscope equipped with a 100×, 1. 25 NA and a 63×, 1.4 NA objectives and a filter wheel combination (Chroma Technology Corp.). Images were collected at one-minute intervals with a CoolSnap HQ camera (Photometrics) controlled through a Metamorph software (Universal imaging); eleven fluorescence optical sections were captured at 1-μm z steps. Movies were created using the Metamorph software and each frame shows the maximum-intensity projection of all the sections.

Immunoprecipitation and western blotting

For immunoblotting analysis of GFP-Cog7 and GFP-Fws, 40 adult testes from males of each genotype, were homogenised in 100 μl of Lysis buffer (10 mM Tris-HCl pH 7.5, 150 mM NaCl, 0.5 mM EDTA, 0.5% NP40, 1 mM PMSF, 1× Protease inhibitor Cocktail) at 4℃. Immunoprecipitation experiments from adult testes expressing GFP- and/or RFP-tagged proteins, were performed using the GFP/RFP trap-A kits and control beads purchased from ChromoTek (Planegg-Martinsried). At least 200 adult testes were homogenised in 500 μl of Lysis buffer at 4℃. Lysates were cleared by centrifugation and protein concentration was quantified using the Bradford protein assay (Bio-Rad, Hercules, CA). 4% of each sample was retained as the 'input', the remainder was incubated with 20 μl of either GFP trap-A/RFP trap-A or control beads for two hours at 4℃. In all cases beads were washed three times and bound proteins were eluted by boiling in SDS

sample buffer. For immunoblots, samples, were separated on 4–20% SDS polyacrylammide precast gels (Bio-Rad) and blotted to PVDF membranes. Blocking and antibody incubation were in Tris-buffered saline (Sigma-Aldrich) with 0,05% Tween-20 (TBST) containing 4% nonfat dry milk (Bio-Rad; Blotting GradeBlocker). Primary antibodies were as follows: anti-Giotto (Giansanti et al., 2006) diluted 1:8000; rat monoclonal anti-RFP (Chromotek, 5F8) diluted 1:1000. GFP was detected using a peroxidase labelled anti-GFP (Vector Laboratories). HRP-linked secondary antibodies (GE Healthcare) were used at 1:5000. After incubation with the antibodies, blots were washed in TBST and imaged using ECL detection kit (GE Healthcare).

Acknowledgements

We thank Rebecca Farkas for the isolation of *z-2805* and *z-5797* mutant lines; J. A. Brill and R. Piergentili for critical reading of the manuscript; G. D. Raffa for technical advices; J. Wakefield, R. Karess and S. Cohen for fly stocks; O. Papoulas, R. Karess, D. B. Roberts, C. Field and W. Trimble for antibodies.

Funding

This work was supported by a grant from Associazione Italiana per la Ricerca sul Cancro, AIRC [grant number IG 10775 to M.G.G.].

Supplementary material available online at
http://jcs.biologists.org/lookup/suppl/doi:10.1242/jcs.108878/-/DC1

References

Albertson, R., Riggs, B. and Sullivan, W. (2005). Membrane traffic: a driving force in cytokinesis. *Trends Cell Biol.* **15**, 92-101.

Albertson, R., Cao, J., Hsieh, T. S. and Sullivan, W. (2008). Vesicles and actin are targeted to the cleavage furrow via furrow microtubules and the central spindle. *J. Cell Biol.* **181**, 777-790.

Boucrot, E. and Kirchhausen, T. (2007). Endosomal recycling controls plasma membrane area during mitosis. *Proc. Natl. Acad. Sci. USA* **104**, 7939-7944.

Brill, J. A., Hime, G. R., Scharer-Schuksz, M. and Fuller, M. T. (2000). A phospholipid kinase regulates actin organization and intercellular bridge formation during germline cytokinesis. *Development* **127**, 3855-3864.

Bruinsma, P., Spelbrink, R. G. and Nothwehr, S. F. (2004). Retrograde transport of the mannosyltransferase Och1p to the early Golgi requires a component of the COG transport complex. *J. Biol. Chem.* **279**, 39814-39823.

Burgess, R. W., Deitcher, D. L. and Schwarz, T. L. (1997). The synaptic protein syntaxin1 is required for cellularization of Drosophila embryos. *J. Cell Biol.* **138**, 861-875.

Chen, D. and McKearin, D. M. (2003). A discrete transcriptional silencer in the bam gene determines asymmetric division of the Drosophila germline stem cell. *Development* **130**, 1159-1170.

Dietzl, G., Chen, D., Schnorrer, F., Su, K. C., Barinova, Y., Fellner, M., Gasser, B., Kinsey, K., Oppel, S., Scheiblauer, S. et al. (2007). A genome-wide transgenic RNAi library for conditional gene inactivation in Drosophila. *Nature* **448**, 151-156.

Dollar, G., Struckhoff, E., Michaud, J. and Cohen, R. S. (2002). Rab11 polarization of the Drosophila oocyte: a novel link between membrane trafficking, microtubule organization, and oskar mRNA localization and translation. *Development* **129**, 517-526.

Dyer, N., Rebollo, E., Domínguez, P., Elkhatib, N., Chavrier, P., Daviet, L., González, C. and González-Gaitán, M. (2007). Spermatocyte cytokinesis requires rapid membrane addition mediated by ARF6 on central spindle recycling endosomes. *Development* **134**, 4437-4447.

Eggert, U. S., Kiger, A. A., Richter, C., Perlman, Z. E., Perrimon, N., Mitchison, T. J. and Field, C. M. (2004). Parallel chemical genetic and genome-wide RNAi screens identify cytokinesis inhibitors and targets. *PLoS Biol.* **2**, e379.

Fabian, L., Wei, H. C., Rollins, J., Noguchi, T., Blankenship, J. T., Bellamkonda, K., Polevoy, G., Gervais, L., Guichet, A., Fuller, M. T. et al. (2010). Phosphatidylinositol 4,5-bisphosphate directs spermatid cell polarity and exocyst localization in Drosophila. *Mol. Biol. Cell* **21**, 1546-1555.

Farkas, R. M., Giansanti, M. G., Gatti, M. and Fuller, M. T. (2003). The Drosophila Cog5 homologue is required for cytokinesis, cell elongation, and assembly of specialized Golgi architecture during spermatogenesis. *Mol. Biol. Cell* **14**, 190-200.

Field, C. M. and Alberts, B. M. (1995). Anillin, a contractile ring protein that cycles from the nucleus to the cell cortex. *J. Cell Biol.* **131**, 165-178.

Foulquier, F., Vasile, E., Schollen, E., Callewaert, N., Raemaekers, T., Quelhas, D., Jaeken, J., Mills, P., Winchester, B., Krieger, M. et al. (2006). Conserved oligomeric Golgi complex subunit 1 deficiency reveals a previously uncharacterized congenital disorder of glycosylation type II. *Proc. Natl. Acad. Sci. USA* **103**, 3764-3769.

Foulquier, F., Ungar, D., Reynders, E., Zeevaert, R., Mills, P., García-Silva, M. T., Briones, P., Winchester, B., Morelle, W., Krieger, M. et al. (2007). A new inborn error of glycosylation due to a Cog8 deficiency reveals a critical role for the Cog1-Cog8 interaction in COG complex formation. *Hum. Mol. Genet.* **16**, 717-730.

Fuller, M. T. (1993). Spermatogenesis. In *The Development of Drosophila melanogaster* (ed. M. Bate and A. Martinez-Arias), pp 71-147. Cold Spring Harbor, NY: Cold Spring Harbor Press.

Gatt, M. K. and Glover, D. M. (2006). The Drosophila phosphatidylinositol transfer protein encoded by vibrator is essential to maintain cleavage-furrow ingression in cytokinesis. *J. Cell Sci.* **119**, 2225-2235.

Giansanti, M. G., Bonaccorsi, S. and Gatti, M. (1999). The role of anillin in meiotic cytokinesis of Drosophila males. *J. Cell Sci.* **112**, 2323-2334.

Giansanti, M. G., Sechi, S., Frappaolo, A., Belloni, G. and Piergentili, R. (2012). Cytokinesis in Drosophila male meiosis. *Spermatogenesis* **2**, 185-196.

Giansanti, M. G., Farkas, R. M., Bonaccorsi, S., Lindsley, D. L., Wakimoto, B. T., Fuller, M. T. and Gatti, M. (2004). Genetic dissection of meiotic cytokinesis in Drosophila males. *Mol. Biol. Cell* **15**, 2509-2522.

Giansanti, M. G., Bonaccorsi, S., Kurek, R., Farkas, R. M., Dimitri, P., Fuller, M. T. and Gatti, M. (2006). The class I PITP giotto is required for Drosophila cytokinesis. *Curr. Biol.* **16**, 195-201.

Giansanti, M. G., Belloni, G. and Gatti, M. (2007). Rab11 is required for membrane trafficking and actomyosin ring constriction in meiotic cytokinesis of Drosophila males. *Mol. Biol. Cell* **18**, 5034-5047.

Inoue, Y. H., Savoian, M. S., Suzuki, T., Máthé, E., Yamamoto, M. T. and Glover, D. M. (2004). Mutations in orbit/mast reveal that the central spindle is comprised of two microtubule populations, those that initiate cleavage and those that propagate furrow ingression. *J. Cell Biol.* **166**, 49-60.

Jones, S. M., Alb, J. G., Jr, Phillips, S. E., Bankaitis, V. A. and Howell, K. E. (1998). A phosphatidylinositol 3-kinase and phosphatidylinositol transfer protein act synergistically in formation of constitutive transport vesicles from the trans-Golgi network. *J. Biol. Chem.* **273**, 10349-10354.

Kingsley, D. M., Kozarsky, K. F., Segal, M. and Krieger, M. (1986). Three types of low density lipoprotein receptor-deficient mutant have pleiotropic defects in the synthesis of N-linked, O-linked, and lipid-linked carbohydrate chains. *J. Cell Biol.* **102**, 1576-1585.

Kondylis, V. and Rabouille, C. (2009). The Golgi apparatus: lessons from Drosophila. *FEBS Lett.* **583**, 3827-3838.

Kranz, C., Ng, B. G., Sun, L., Sharma, V., Eklund, E. A., Miura, Y., Ungar, D., Lupashin, V., Winkel, R. D., Cipollo, J. F. et al. (2007). COG8 deficiency causes new congenital disorder of glycosylation type IIh. *Hum. Mol. Genet.* **1**, 731-741.

Laufman, O., Hong, W. and Lev, S. (2011). The COG complex interacts directly with Syntaxin 6 and positively regulates endosome-to-TGN retrograde transport. *J. Cell Biol.* **194**, 459-472.

Loh, E. and Hong, W. (2004). The binary interacting network of the conserved oligomeric Golgi tethering complex. *J. Biol. Chem.* **279**, 24640-24648.

Lübbehusen, J., Thiel, C., Rind, N., Ungar, D., Prinsen, B. H., de Koning, T. J., van Hasselt, P. M. and Körner, C. (2010). Fatal outcome due to deficiency of subunit 6 of the conserved oligomeric Golgi complex leading to a new type of congenital disorders of glycosylation. *Hum. Mol. Genet.* **19**, 3623-3633.

McKay, H. F. and Burgess, D. R. (2011). 'Life is a highway': membrane trafficking during cytokinesis. *Traffic* **12**, 247-251.

Morava, E., Zeevaert, R., Korsch, E., Huijben, K., Wopereis, S., Matthijs, G., Keymolen, K., Lefeber, D. J., De Meirleir, L. and Wevers, R. A. (2007). A common mutation in the COG7 gene with a consistent phenotype including microcephaly, adducted thumbs, growth retardation, VSD and episodes of hyperthermia. *Eur. J. Hum. Genet.* **15**, 638-645. body, and motile cilium assembly. *Mol. Biol. Cell* **20**, 2605-2614.

Neto, H., Collins, L. L. and Gould, G. W. (2011). Vesicle trafficking and membrane remodelling in cytokinesis. *Biochem. J.* **437**, 13-24.

Ng, M. M., Chang, F. and Burgess, D. R. (2005). Movement of membrane domains and requirement of membrane signaling molecules for cytokinesis. *Dev. Cell* **9**, 781-790.

Ng, B. G., Kranz, C., Hagebeuk, E. E., Duran, M., Abeling, N. G., Wuyts, B., Ungar, D., Lupashin, V., Hartdorff, C. M., Poll-The, B. T. et al. (2007). Molecular and clinical characterization of a Moroccan Cog7 deficient patient. *Mol. Genet. Metab.* **91**, 201-204.

Niswonger, M. L. and O'Halloran, T. J. (1997). A novel role for clathrin in cytokinesis. *Proc. Natl. Acad. Sci. USA* **94**, 8575-8578.

Ohashi, M., Jan de Vries, K., Frank, R., Snoek, G., Bankaitis, V., Wirtz, K. and Huttner, W. B. (1995). A role for phosphatidylinositol transfer protein in secretory vesicle formation. *Nature* **377**, 544-547.

Oka, T., Ungar, D., Hughson, F. M. and Krieger, M. (2004). The COG and COPI complexes interact to control the abundance of GEARs, a subset of Golgi integral membrane proteins. *Mol. Biol. Cell* **15**, 2423-2435.

Oka, T., Vasile, E., Penman, M., Novina, C. D., Dykxhoorn, D. M., Ungar, D., Hughson, F. M. and Krieger, M. (2005). Genetic analysis of the subunit organization and function of the conserved oligomeric golgi (COG) complex: studies of COG5- and COG7-deficient mammalian cells. *J. Biol. Chem.* **280**, 32736-32745.

Paesold-Burda, P., Maag, C., Troxler, H., Foulquier, F., Kleinert, P., Schnabel, S., Baumgartner, M. and Hennet, T. (2009). Deficiency in COG5 causes a moderate form of congenital disorders of glycosylation. *Hum. Mol. Genet.* **18**, 4350-4356.

Peanne, R., Legrand, D., Duvet, S., Mir, A. M., Matthijs, G., Rohrer, J. and Foulquier, F. (2011). Differential effects of lobe A and lobe B of the Conserved Oligomeric Golgi complex on the stability of beta1,4-galactosyltransferase 1 and alpha2,6-sialyltransferase 1. *Glycobiology* **21**, 864-876.

Polevoy, G., Wei, H. C., Wong, R., Szentpetery, Z., Kim, Y. J., Goldbach, P., Steinbach, S. K., Balla, T. and Brill, J. A. (2009). Dual roles for the Drosophila PI 4-kinase four wheel drive in localizing Rab11 during cytokinesis. *J. Cell Biol.* **187**, 847-858.

Prekeris, R. and Gould, G. W. (2008). Breaking up is hard to do - membrane traffic in cytokinesis. *J. Cell Sci.* **121**, 1569-1576.

Rabouille, C., Kuntz, D. A., Lockyer, A., Watson, R., Signorelli, T., Rose, D. R., van den Heuvel, M. and Roberts, D. B. (1999). The Drosophila GMII gene encodes a Golgi alpha-mannosidase II. *J. Cell Sci.* **112**, 3319-3330.

Raffa, G. D., Raimondo, D., Sorino, C., Cugusi, S., Cenci, G., Cacchione, S., Gatti, M. and Ciapponi, L. (2010). Verrocchio, a Drosophila OB fold-containing protein, is a component of the terminin telomere-capping complex. *Genes Dev.* **24**, 1596-1601.

Ram, R. J., Li, B. and Kaiser, C. A. (2002). Identification of Sec36p, Sec37p, and Sec38p: components of yeast complex that contains Sec34p and Sec35p. *Mol. Biol. Cell* **13**, 1484-1500.

Reddy, P. and Krieger, M. (1989). Isolation and characterization of an extragenic suppressor of the low-density lipoprotein receptor-deficient phenotype of a Chinese hamster ovary cell mutant. *Mol. Cell. Biol.* **9**, 4799-4806.

Reynders, E., Foulquier, F., Leão Teles, E., Quelhas, D., Morelle, W., Rabouille, C., Annaert, W. and Matthijs, G. (2009). Golgi function and dysfunction in the first COG4-deficient CDG type II patient. *Hum. Mol. Genet.* **18**, 3244-3256.

Robinett, C. C., Giansanti, M. G., Gatti, M. and Fuller, M. T. (2009). TRAPPII is required for cleavage furrow ingression and localization of Rab11 in dividing male meiotic cells of Drosophila. *J. Cell Sci.* **122**, 4526-4534.

Royou, A., Sullivan, W. and Karess, R. (2002). Cortical recruitment of nonmuscle myosin II in early syncytial Drosophila embryos: its role in nuclear axial expansion and its regulation by Cdc2 activity. *J. Cell Biol.* **158**, 127-137.

Shestakova, A., Zolov, S. and Lupashin, V. V. (2006). COG complex-mediated recycling of Golgi glycosyltransferases is essential for normal protein glycosylation. *Traffic* **7**, 191-204.

Simon, J. P., Morimoto, T., Bankaitis, V. A., Gottlieb, T. A., Ivanov, I. E., Adesnik, M. and Sabatini, D. D. (1998). An essential role for the phosphatidylinositol transfer protein in the scission of coatomer-coated vesicles from the trans-Golgi network. *Proc. Natl. Acad. Sci. USA* **95**, 11181-11186.

Sisson, J. C., Field, C., Ventura, R., Royou, A. and Sullivan, W. (2000). Lava lamp, a novel peripheral golgi protein, is required for Drosophila melanogaster cellularization. *J. Cell Biol.* **151**, 905-918.

Smith, R. D. and Lupashin, V. V. (2008). Role of the conserved oligomeric Golgi (COG) complex in protein glycosylation. *Carbohydr. Res.* **343**, 2024-2031.

Smith, R. D., Willett, R., Kudlyk, T., Pokrovskaya, I., Paton, A. W., Paton, J. C. and Lupashin, V. V. (2009). The COG complex, Rab6 and COPI define a novel Golgi retrograde trafficking pathway that is exploited by SubAB toxin. *Traffic,* **10**, 1502-1517.

Sohda, M., Misumi, Y., Yoshimura, S., Nakamura, N., Fusano, T., Ogata, S., Sakisaka, S. and Ikehara, Y. (2007). The interaction of two tethering factors, p115 and COG complex, is required for Golgi integrity. *Traffic* **8**, 270-284.

Sohda, M., Misumi, Y., Yamamoto, A., Nakamura, N., Ogata, S., Sakisaka, S., Hirose, S., Ikehara, Y. and Oda, K. (2010). Interaction of Golgin-84 with the COG complex mediates the intra-Golgi retrograde transport. *Traffic* **11**, 1552-1566.

Spaapen, L. J., Bakker, J. A., van der Meer, S. B., Sijstermans, H. J., Steet, R. A., Wevers, R. A. and Jaeken, J. (2005). Clinical and biochemical presentation of siblings with COG-7 deficiency, a lethal multiple O- and N-glycosylation disorder. *J. Inherit. Metab. Dis.* **28**, 707-714.

Steet, R. and Kornfeld, S. (2006). COG-7-deficient human fibroblasts exhibit altered recycling of Golgi proteins. *Mol. Biol. Cell* **17**, 2312-2321.

Suvorova, E. S., Kurten, R. C. and Lupashin, V. V. (2001). Identification of a human orthologue of Sec34p as a component of the cis-Golgi vesicle tethering machinery. *J. Biol. Chem.* **276**, 22810-22818.

Suvorova, E. S., Duden, R. and Lupashin, V. V. (2002). The Sec34/Sec35p complex, a Ypt1p effector required for retrograde intra-Golgi trafficking, interacts with Golgi SNAREs and COPI vesicle coat proteins. *J. Cell Biol.* **157**, 631-643.

Tates, A. D. (1971). *Cytodifferentiation During Spermatogenesis in Drosophila Melanogaster: an Electron Microscope Study*. PhD thesis, Rijksuniversiteit de Leiden, Leiden, The Netherlands.

Ungar, D., Oka, T., Brittle, E. E., Vasile, E., Lupashin, V. V., Chatterton, J. E., Heuser, J. E., Krieger, M. and Waters, M. G. (2002). Characterization of a mammalian Golgi-localized protein complex, COG, that is required for normal Golgi morphology and function. *J. Cell Biol.* **157**, 405-415.

Ungar, D., Oka, T., Krieger, M. and Hughson, F. M. (2006). Retrograde transport on the COG railway. *Trends Cell Biol.* **16**, 113-120.

VanRheenen, S. M., Cao, X., Lupashin, V. V., Barlowe, C. and Waters, M. G. (1998). Sec35p, a novel peripheral membrane protein, is required for ER to Golgi vesicle docking. *J. Cell Biol.* **141**, 1107-1119.

VanRheenen, S. M., Cao, X., Sapperstein, S. K., Chiang, E. C., Lupashin, V. V., Barlowe, C. and Waters, M. G. (1999). Sec34p, a protein required for vesicle tethering to the yeast Golgi apparatus, is in a complex with Sec35p. *J. Cell Biol.* **147**, 729-742.

Vasile, E., Oka, T., Ericsson, M., Nakamura, N. and Krieger, M. (2006). IntraGolgi distribution of the Conserved Oligomeric Golgi (COG) complex. *Exp. Cell Res.* **312**, 3132-3141.

Wakimoto, B. T., Lindsley, D. L. and Herrera, C. (2004). Toward a comprehensive genetic analysis of male fertility in Drosophila melanogaster. *Genetics* **167**, 207-216.

Walter, D. M., Paul, K. S. and Waters, M. G. (1998). Purification and characterization of a novel 13 S hetero-oligomeric protein complex that stimulates *in vitro* Golgi transport. *J. Biol. Chem.* **273**, 29565-29576.

Wei, H. C., Rollins, J., Fabian, L., Hayes, M., Polevoy, G., Bazinet, C. and Brill, J. A. (2008). Depletion of plasma membrane PtdIns(4,5)P2 reveals essential roles for phosphoinositides in flagellar biogenesis. *J. Cell Sci.* **121**, 1076-1084.

Whyte, J. R. and Munro, S. (2001). The Sec34/35 Golgi transport complex is related to the exocyst, defining a family of complexes involved in multiple steps of membrane traffic. *Dev. Cell* **1**, 527-537.

Wu, X., Steet, R. A., Bohorov, O., Bakker, J., Newell, J., Krieger, M., Spaapen, L., Kornfeld, S. and Freeze, H. H. (2004). Mutation of the COG complex subunit gene COG7 causes a lethal congenital disorder. *Nat. Med.* **10**, 518-523.

Wuestehube, L. J., Duden, R., Eun, A., Hamamoto, S., Korn, P., Ram, R. and Schekman, R. (1996). New mutants of Saccharomyces cerevisiae affected in the transport of proteins from the endoplasmic reticulum to the Golgi complex. *Genetics* **142**, 393-406.

Xu, H., Brill, J. A., Hsien, J., McBride, R., Boulianne, G. L. and Trimble, W. S. (2002a). Syntaxin 5 is required for cytokinesis and spermatid differentiation in Drosophila. *Dev. Biol.* **251**, 294-306.

Xu, H., Boulianne, G. L. and Trimble, W. S. (2002b). Drosophila syntaxin 16 is a Q-SNARE implicated in Golgi dynamics. *J. Cell Sci.* **115**, 4447-4455.

Yoshigaki, T. (1997). Accumulation of WGA receptors in the cleavage furrow during cytokinesis of sea urchin eggs. *Exp. Cell Res.* **236**, 463-471.

Zhou, X., Fabian, L., Bayraktar, J. L., Ding, H. M., Brill, J. A. and Chang, H. C. (2011). Auxilin is required for formation of Golgi-derived clathrin-coated vesicles during Drosophila spermatogenesis. *Development* **138**, 1111-1120.

Zolov, S. N. and Lupashin, V. V. (2005). Cog3p depletion blocks vesicle-mediated Golgi retrograde trafficking in HeLa cells. *J. Cell Biol.* **168**, 747-759.

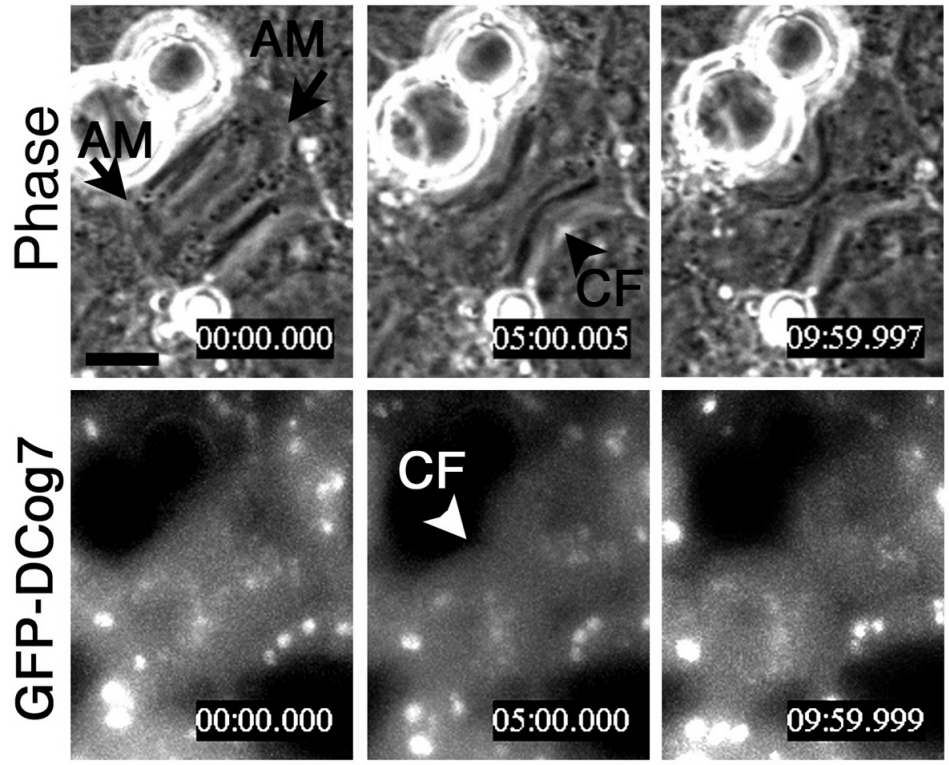

Fig. S1. Cog7 does not accumulate at the cleavage site of telophase spermatocytes. Selected frames (Phase contrast and corresponding fluorescence images) of a time lapse from a spermatocyte expressing GFP-Cog7 undergoing telophase. GFP does not accumulate at the cleavage furrows (CF). Bar, 10♣∀m.

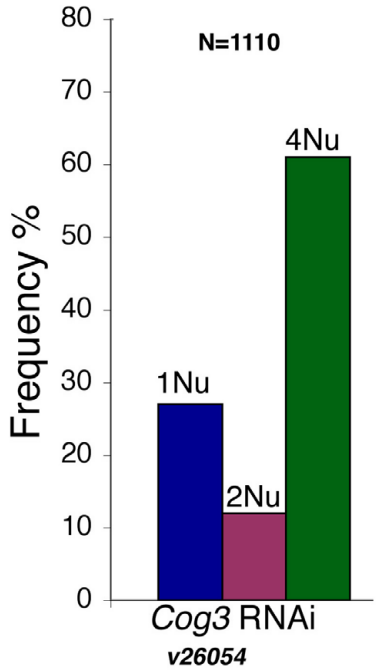

Fig. S2. Frequencies of spermatids containing 1, 2, or 4 nuclei per each NK in testes from males expressing dsRNA against *CG3248*, the *Drosophila Cog3 (Cog3)*. *UAS::DCog3-RNAi* was expressed in male meiosis using Bam-GAL4 (Chen and McKearin, 2003). The frequency of multinucleate spermatids in the Bam-GAL4 stock (used as a control) was zero.

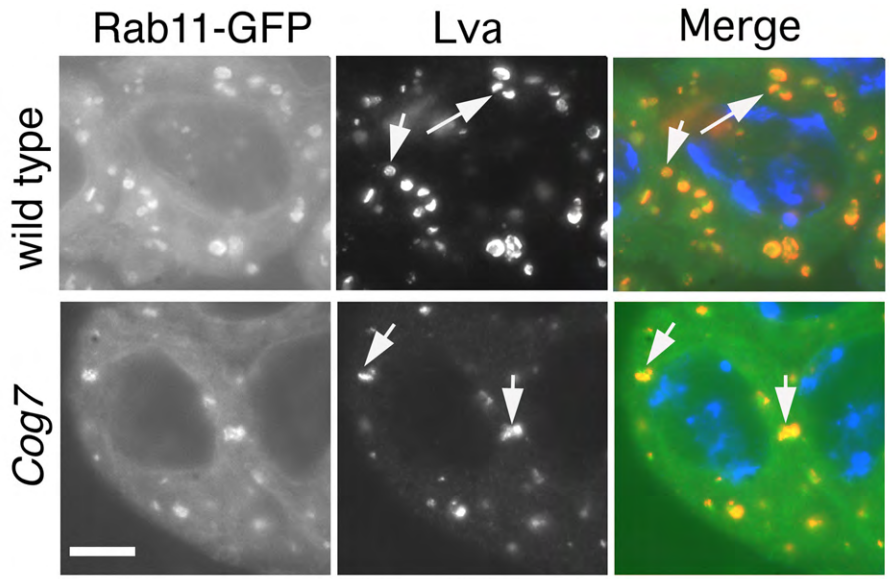

Fig. S3. Localisation of Rab11-GFP in prophase spermatocytes from wild type and *Cog7* males. Prophase spermatocytes expressing Rab11-GFP (green) were fixed and stained for Lva (red) and DNA (blue). Arrows point to Golgi stacks. Bar, 10♣∀m

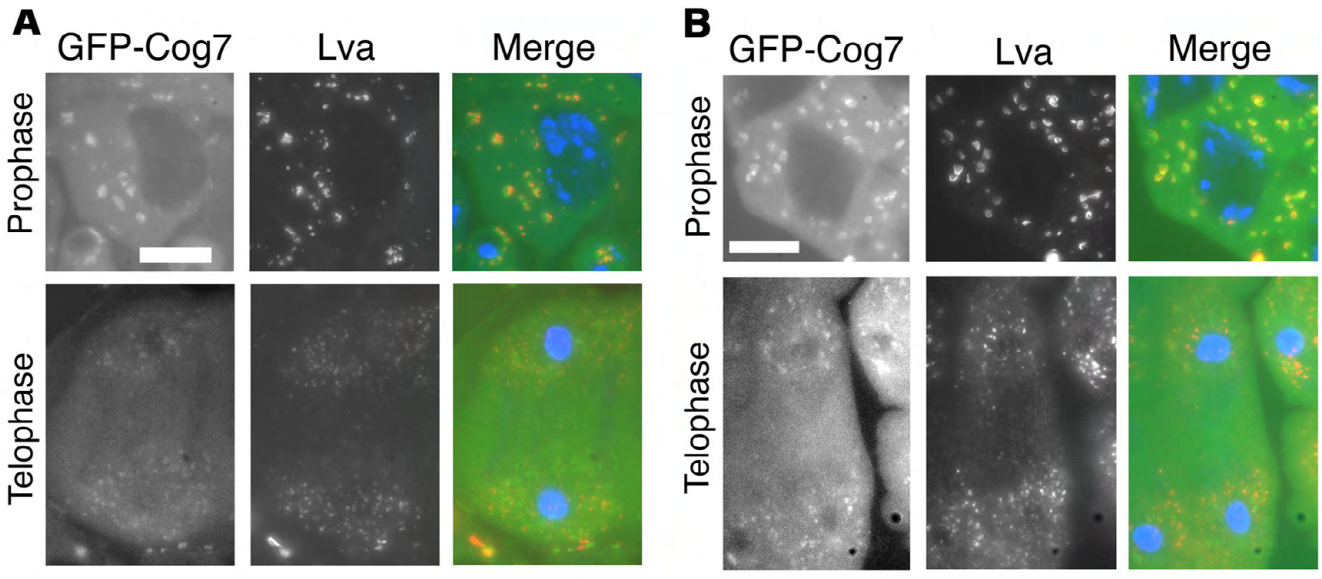

Fig. S4. Localisation of GFP-Cog7 in spermatocytes from *gio* and *Rab11* is comparable to wild type. Spermatocytes expressing GFP-Cog7 (green) from GFP-Cog7; $gio^{z3934}/Df(3R)D1\text{-}BX12$ (A) and GFP-Cog7; $Rab11^{e(To)11}/Rab11^{93Bi}$ (B) males were fixed and stained for Lva (red) and DNA (blue). Bar, 10♣∀m

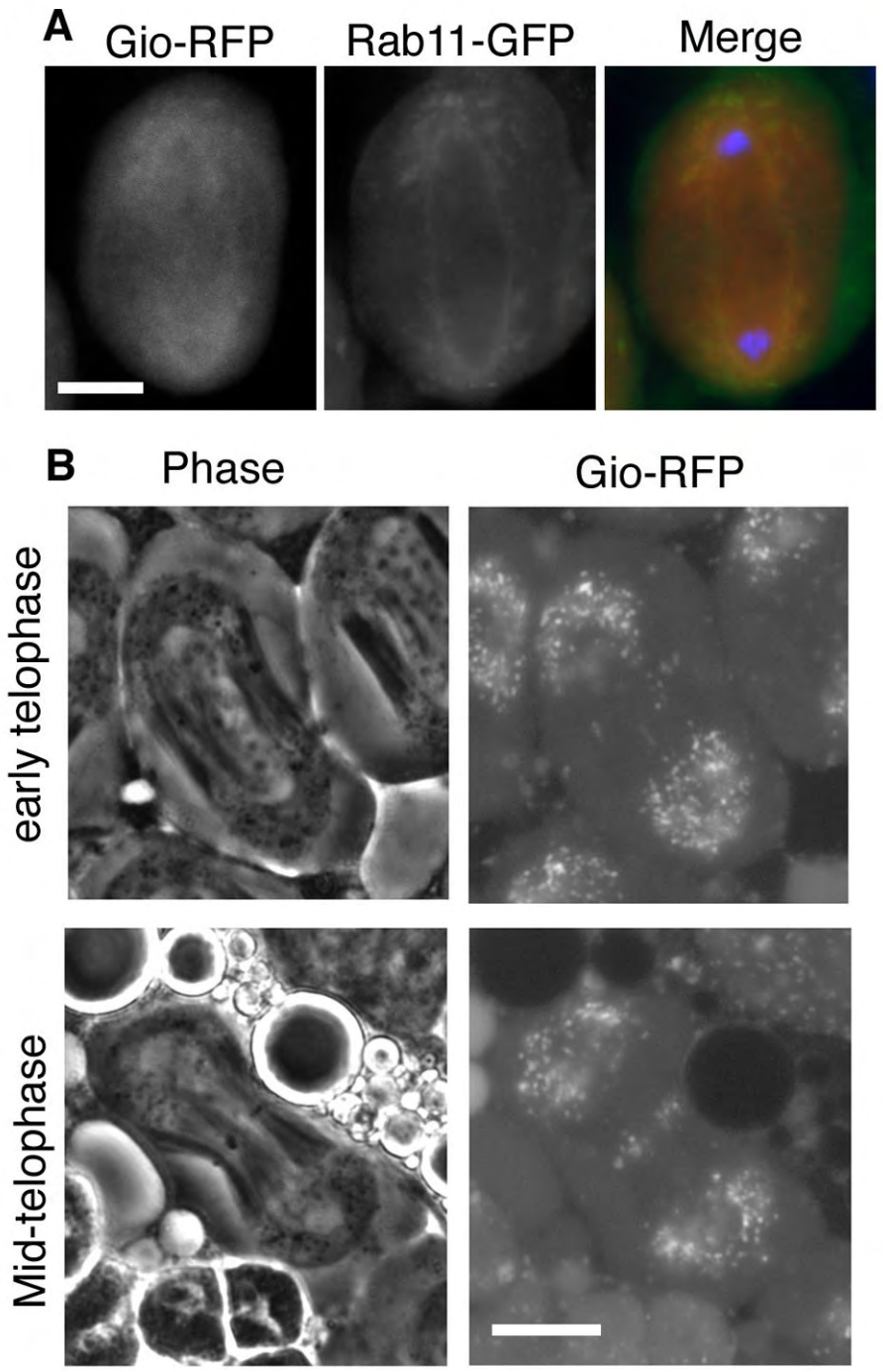

Fig. S5. Gio-RFP colocalizes with Rab11-GFP in dividing spermatocytes and concentrates at the cleavage furrow during telophase. (A) Spermatocyte expressing both Rab11-GFP (green) and Gio-RFP (red), were fixed and stained for DNA (blue). (B) Live dividing spermatocytes expressing Gio-RFP during early telophase and mid-telophase. Panels show phase contrast images (Phase) and corresponding fluorescence images. Bar, 10♣∀m

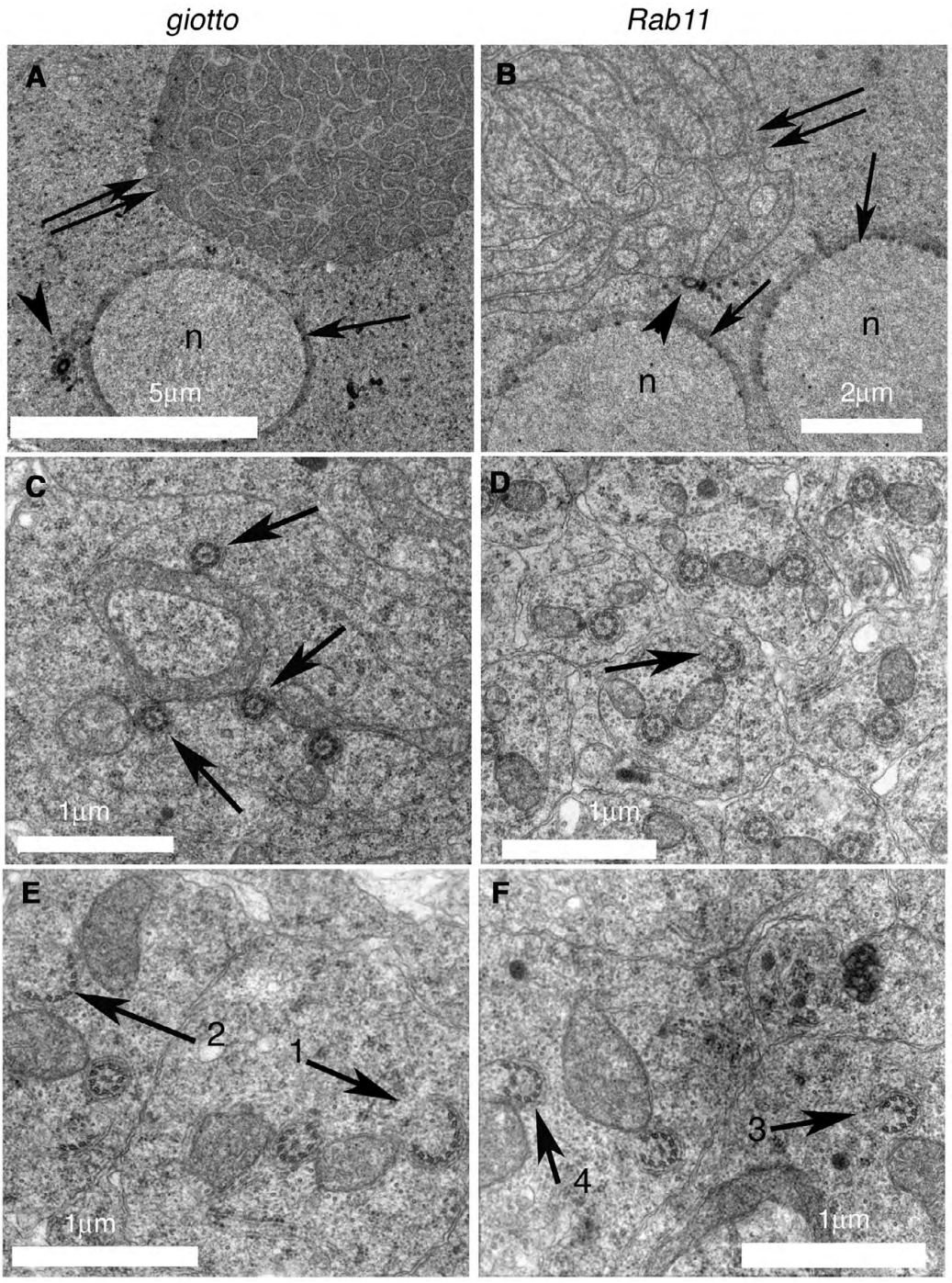

Fig. S6. Spermatids from *gio* and *Rab11* males display defects in basal body docking and axonemal structure. (A,B) TEM micrographs from *gio*^{z3934}/*Df(3R)D1-BX12* (A) and *Rab11*$^{e(To)11}$/*Rab11*^{93Bi} (B) spermatids. Arrowheads in A and B point to basal bodies. Nuclei (n), nuclear envelopes (arrow) and mitochondrial derivatives (double arrows) are indicated. (C–F) TEM micrographs showing axonemes in *gio*^{z3934}/*Df(3R)D1-BX12* (C,E) and *Rab11*$^{e(To)11}$/*Rab11*^{93Bi} (D,F) mutant spermatids. (C) Arrows point to three regular axonemes associated with a large mitochondrial derivative. (D) Arrow points to an irregular axoneme that lacks two peripheral doublets. (E,F) One axoneme in E lacks internal central microtubules (1, arrow). Other axonemes exhibit an irregular splayed structure (2, 3, 4 arrows).

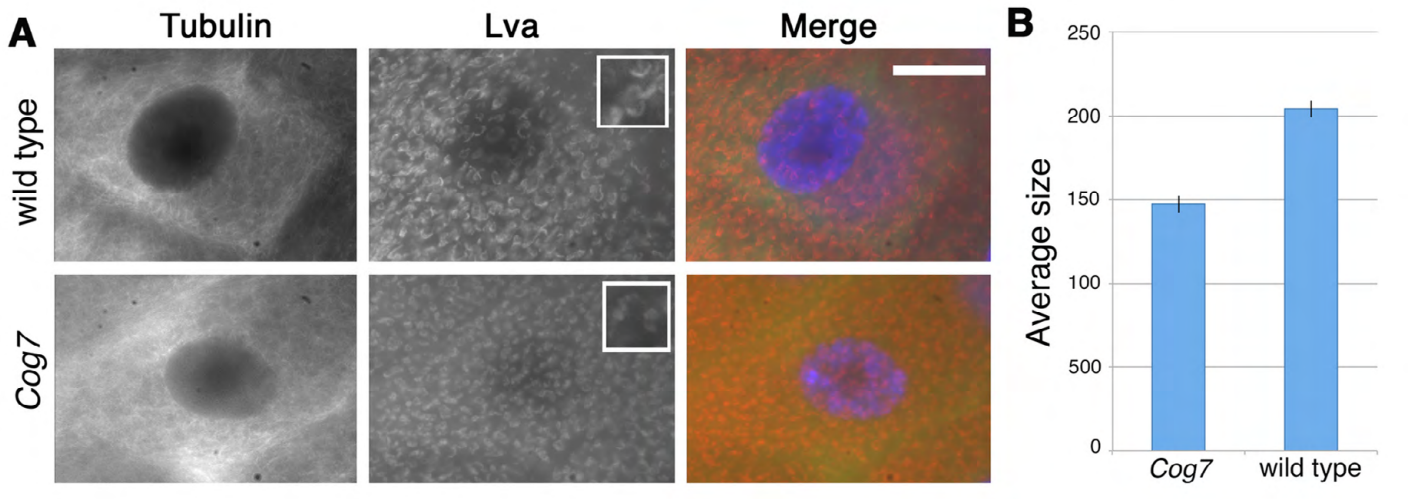

Fig. S7. Loss of Cog7 affects the size of Golgi in larval salivary gland cells. (A) Salivary glands were stained for Lva (red), tubulin (green) and DNA (blue). Insets show higher magnifications. (B) Average area of Golgi bodies (+/– SEM) expressed in arbitrary units.